



Llgl1 regulates zebrafish cardiac development by mediating Yap stability in cardiomyocytes

Michael A. Flinn, Cécile Otten, Zachary J. Brandt, Jonathan R. Bostrom, Aria Kenarsary, Tina C. Wan, John A. Auchampach, Salim Abdelilah-Seyfried, Caitlin C. O'Meara and Brian A. Link

DOI: 10.1242/dev.193581

Editor: Benoit Bruneau

Review timeline

Original submission: 5 June 2020

Accepted: 10 July 2020

Original submission

First decision letter

MS ID#: DEVELOP/2020/193581

MS TITLE: Llgl1 regulates zebrafish cardiac development by mediating Yap stability in cardiomyocytes

AUTHORS: Michael A. Flinn, Cécile Otten, Zachary J. Brandt, Jonathan R. Bostrom, Aria Kenarsary, Tina C. Wan, John A. Auchampach, Salim Abdelilah-Seyfried, Caitlin C. O'Meara, and Brian A. Link

ARTICLE TYPE: Research Article

Dear Dr. Link

I am happy to tell you that your manuscript has been accepted for publication in Development, pending our standard ethics checks. You will see that we enlisted a new reviewer, who was somewhat negative. However, their comments largely centred on image presentation, were not shared by the original reviewer, and I also don't have an issue with them.

Reviewer 1

Advance summary and potential significance to field

In this manuscript, Brian Link and colleagues describe a role for the Lethal giant larvae family member Llgl1 in zebrafish valve development and modulation of Hippo signalling. Studies in *Drosophila* and vertebrate models have uncovered functions for Llgl1 in apical membrane polarity and regulation of Notch and Hippo signalling. In particular, *l(2)gl* mutation in flies leads to excessive Yorkie-mediated transcriptional outputs.

Both Notch and Hippo signalling pathways play important roles in heart development, with restriction of Notch activity to the atrioventricular canal (AVC) being essential for valve formation, and levels of Taz/Yap activity regulating cardiomyocyte cell number and heart size.

Given the known roles for Notch and Hippo signalling in heart development, and the previous description of overt cardiac defects in *llgl1*-depleted zebrafish embryos, the authors first examined the effects of *llgl1/2* knockdown (siRNA) in neonatal rat cardiomyocytes. Decreased Yap protein levels and expression of Yap transcriptional targets were observed following knockdown of either Llgl1 or 2. In *llgl1* mutant zebrafish, epidermal defects are correlated with decreased Yap protein levels. Cardiac defects are also observed, including retrograde blood flow and a failure to restrict

Notch activity to the AVC, resulting in defective EMT and valve cushion formation. Preliminary data suggests that restoration of Yap may overcome some aspects of cardiac defects following knockdown of *llg1*.

Overall, this work shows an interesting linkage between vertebrate *Llgl1* and Yap levels that is opposite of what is described in *Drosophila*. This may reflect differences, as noted by the authors, in the presence of a Lats-targeted phosphodegron sequence in Yap (but not Yorkie). These results further validate and extend previous morpholino-based analysis of *llg1* phenotypes in zebrafish, and characterize novel cardiac phenotypes.

Comments for the author

The authors have addressed my comments, and added an appreciable amount of data on analysis of cardiac phenotypes following *Llgl1* loss.

Reviewer 2

Advance summary and potential significance to field

In this manuscript, Flinn et al. describe a novel role for *Llgl1* both in regulating Yap stability and in cardiac morphogenesis. Benefitting from rat cardiomyocyte cell culture, the authors first demonstrate decreased levels of Yap protein following knockdown of *Llgl1* and its paralogue, *Llgl2*. Their recently generated TALENs *llg1*^{-/-} embryos exhibit pericardial effusion which the authors propose is secondary to defects in Yap localization and apical junction remodeling. Phenotypic assessment of the embryonic and adult *llg1* mutants highlights abnormal looping, cardiomyocyte hypertrophy, and perturbed cardiac hemodynamics. In addition to the visualization of retrograde blood flow through the atrioventricular (AV) canal, the use of a Notch1 reporter line illustrates an expanded region of notch-responsiveness along the AV valve of *llg1*^{-/-} embryos.

The authors next show Yap expression in zebrafish cardiomyocytes and partial rescue of the pericardial edema phenotype upon cardiomyocyte-specific overexpression of Yap. Finally, in the zebrafish epidermis injection of eGFP-Yap fusion proteins into *llg1* morphants reveals impaired Yap membrane localization suggesting a potential role for loss of *Llgl1* in remodeling of apical junctions in epithelia and intercalated discs in cardiomyocytes.

This reviewer appreciates the novelty in describing a new zebrafish *llg1* mutant with cardiovascular defects. However, the authors do not dissect the embryonic nor the adult phenotype with adequate experimental rigor. Furthermore, while the cardiomyocyte-specific rescue points to a role for *Llgl1* in normal cardiac morphogenesis, the additional mechanistic experiments evaluating Yap stability are not sufficient to reinforce the requirement of *Llgl1* in mediating Yap protein levels in the heart. In light of these concerns, this manuscript is not appropriate for the Development readership.

Comments for the author

Major Issues:

1. Regarding the experiments described in Figure 1, it is unclear why the authors did not determine the effect of siRNA treatment against both *Llgl1* and *Llgl2* on the Yap protein levels in rat cardiomyocytes given that the qRT-PCR results were noted in this condition. Furthermore, it would be helpful to understand why the authors did not pursue the study of *llg2* loss-of-function and the double knock down (*llg1* and *llg2*) given the qRT-PCR findings.

2. While the variable expressivity of the cardiac phenotype was addressed experimentally, there was no hypothesis provided to explain this dramatic range in severity. Furthermore, a detailed discussion of the natural history of the moderately and severely affected *llg1*^{-/-} embryos would be helpful. Was a time series/natural history experiment performed of individual embryos between 3 and 5 dpf to clarify the disease progression? Also, in Figure 2D, given the genetic cross, it appears that the Mendelian prediction for survival should be 50%. However, the dotted line is not consistent with this expectation.

3. In Figure 3, the authors demonstrate cardiac defects in the *llgl1*^{-/-} embryos. First, the images in panel A should be acquired from a more rostral position in order to visualize the atrium and ventricle en face.

Otherwise, true laterality is difficult to assess. Second, it would be helpful to demonstrate the chamber-specific cell counting strategy with images comparing the wild-type and mutant hearts. Third, why are only the distances between the atrial CM nuclei assessed in panel C (as opposed to the ventricular CMs)? A finding of ventricular CM hypertrophy would have more significance than atrial CM hypertrophy. Finally, it is unclear why the authors would represent a cardiac looping defect in a different imaging modality for the mutants (panel D) when compared to the morphants.

4. While this reviewer appreciates the benefits of echocardiographic evaluation in adult zebrafish hearts there are several technical strategies that are confusing:

- Why was the stroke volume not normalized to body length when the EDV and ESV were?
- The parameters used address volume status. However, the authors draw conclusions about cardiac function from this figure.
- If the authors intend to define a defect in cardiac muscle relaxation, E/A reversal would be the most appropriate measure.

5. Although the authors explain their rationale for use of the *llgl1* morphants rather than *llgl1*^{-/-} embryos *llgl1* morphants are employed in many experiments in which microinjections are not required. This inconsistency in the methodology leads to significant confusion in the flow of the manuscript and diminishes the impact of the data.

6. In Figure 6, while the demonstration of Yap protein expression in ventricular cardiomyocytes is elegant the confocal images are not presented in a standard view and are somewhat confusing to the reader.

Furthermore, in line 373, the authors mention that the ventricular size was measured, and those data are not represented in the associated figure nor are they relevant to these panels. Finally, the use of pericardial edema and blood flow as a measure of rescue is less specific than demonstrating improvement in cellular aspects of the phenotype (as illustrated in Fig. 3). From this perspective, the significance of the overall conclusion from these results is minimized.

7. In Figure 7, although the authors make an argument for extrapolation of the membrane localization findings from the epidermis to the cardiomyocytes, it is unclear why these experiments were not attempted in the heart. With either sectioning or dissection, would adequate visualization of the cardiomyocyte-specific Yap expression be achieved? If the authors experienced challenges with this approach, it would be enlightening to understand the roadblocks.

Minor Issues:

1. There are several places in the manuscript where the wording is repetitive (see lines 353-355, for example).
2. In line 419, I believe that the word should be “rendering”.
3. There are a few examples of inconsistent terminology (see lines 476-477, for example).

First revision

Author response to reviewers' comments

We thank the Editors and Reviewers for their time and thoughtful comments. In order to strengthen our manuscript, we have addressed the Reviewers' concerns through additional experiments and modifications to the manuscript as described below. We have significantly refocused the manuscript to characterize *Lgl1*'s role regulating Yap protein expression and activity in cardiomyocytes and we have further investigated cardiac phenotypic consequences of

Llgl1 depletion. Each Reviewer's comments are addressed individually, even if redundant with previous comments from different Reviewers.

Reviewer 1

1. In Figure 2, it would be useful to show the nature of the protein product made following the deletion in Exon 1. Can alternative transcripts be made? Was qRT-PCR carried out to examine this?

Author Response: The reviewer makes a valid point as we previously did not show the predicted protein product or decreased Llgl1 expression in our mutant line. We now provide a schematic representation of the predicted llgl1 protein product following deletion in Exon 1 in **Figure S1**:

llgl1 wildtype protein

```
MMKFRFRRQGNDPHREKIKQDLFAFNKTVEHGFPNQPSALAYDPKLQLMAIGTKSGAIKIYGAPGVEMTG
LHKDTAAVTQIHFLCGQGRIISLDDNTIHLWEIVQRENRSLLLEVHVSFNLPGRPGIESTSATRVTVMLL
NLSCNLLALGTEGGGVHFLELPTLTLNLSLQDEIMQSVPEEYKCGKSLGPVESLQEHPKDSDKILIGY
SRGLVVLWDLSSRHVDNLFGLGKQQLESVWERSGNSFVSSHSDGGYMWAVSSSNPCTHDPVSSSTIPIYGP
FPCKAVNKILWRTTESGAPLVLFSGGMPRASYGDRHCLTILQDSSHVTLDFTSRVIDFFTIHCTDTEKDF
DEPSALVVLLLEELVVIDLQMPGWPTVPAPYLAPLHSSAITCSCHISNVPPKLWERVISAGQQQCPLQNY
ENWPICGGKNLAPDPKQKELLLTGHEGTVRFWDASGVSLKPLYKLSTASIFQTDCEHNDSLQAGEEEW
PPFRKVGCFDPYSDDPRLGIQKISLCKYSGKLVVAGTAGQVIVMVLGDEKSDHMI DVATVDLLQDREGFT
WKGHDLRPPKSGSVVFAPGFQPVVLVQCLPPAAVTAVTLHAEWNLIAFGTSHGFGLFDYHRRSPVLARCT
LHPNDSLAMEGPLSRVKSLLKSLRQSFRRIRKSRVSGKKRVVNSPTSKVQEANAHLDHDAEVTVPVQRR
IEPRSADDLSLGVVRCCLCFADTFLRDGTHHGPTMWAGTNSGVSVAAYALDVPSQEFSEQSVEALLGKEIQ
LMHRAPVVSIAVLDGRGNPLPEPEYVSRDLAKAPDMQGSVLIASEEQFKVFMLPKVSAKTKFKLTAHE
GCRVRKVALANFTSVSSEYSENALVCLTNMGDIHMFVSPALRPQVRYDCVRKEDISGIASCVFTKTGQG
FYLISPSEYERFSLARVITEPLCGVDVERPHDVS AHSSSTLPPQANGTHKSQAESKSAETEDLLEEMR
SVLSSPILDSPNSSADITLDTTGDLTVEDVKDFLMTVDEAENNFNITEEDGRSAGILIN
```

llgl1^{mw83} (c. 55_64del) product

```
MMKFRFRRQGNDPHREKICLHSIRQLNMDFQTSQVLWPMIPNCSLWLELNQGPSKYMVLQG
```

“Fig. S1. Llgl1 protein sequences. Amino acid sequences for products of wildtype llgl1 of Danio rerio and the llgl1^{mw83} mutant allele. Yellow highlight indicates native amino acid sequence and gray indicates missense amino acid sequence”.

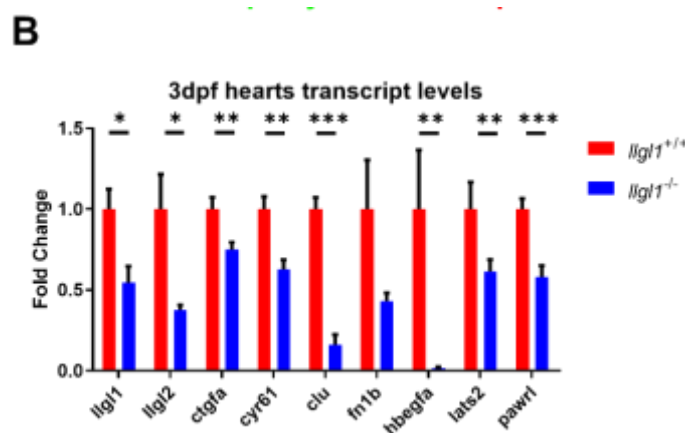
Efforts were made to stain for Llgl1 protein, however we were unable to find a viable antibody for zebrafish. qRT-PCR for llgl1 and llgl2 transcript levels in wildtype and mutant siblings from the llgl1^{mw83} line was performed in response to this reviewer concern. There is statistically *significant depletion of both transcripts in llgl1^{-/-} mutant hearts at 3 dpf as well as decreased expression of transcripts associated with Yap activity. We have clarified this in the Section 3.4:*

“Furthermore, qRT-PCR analysis revealed a decrease of Yap regulated transcripts from hearts isolated from 3 dpf llgl1^{-/-} embryos compared to wildtype (Fig. 6B). Expression of both llgl1 and llgl2 transcripts were also significantly decreased.”

and within the Discussion:

“However, as we could not find a Llgl1 antibody specific for zebrafish, we cannot rule out splicing variants or alternative start sites accounting for some diminished form of Llgl1 expression in llgl1^{mw8} mutant fish. Nonetheless, we show depletion of Llgl1 in cultured rat cardiomyocytes and zebrafish cardiomyocytes and epidermal cells in vivo resulted in lower levels of total Yap protein. Furthermore, depletion of Llgl1 also resulted in diminished expression of Yap-TEAD target genes in both llgl1^{-/-} mutant zebrafish and cultured rat cardiomyocytes.”

and have added this data to **Figure 6B**:



“Fig. 6. *Llgl1* promotes appropriate Yap protein levels in cardiomyocytes and exogenous expression of Yap in cardiomyocytes ameliorates deleterious cardiac physiology associated with loss of *Llgl1* (B) qRT-PCR transcript analysis for *llgl1*, *llgl2* and genes regulated by Yap activity in *llgl1*^{+/+} or *llgl1*^{-/-} 3 dpf zebrafish hearts. n = 10 for each group. Two-tailed unpaired student’s t-test.”

Given these results, while we cannot rule out a potential splice variant accounting for some form of haploinsufficiency, we nonetheless suspect our phenotype is due to lack of functional endogenous *Llgl1*.

2. Some of the data in Figure 3 is confusing as presented. Are these mosaic F0 embryos for the transgenics? If so, why is a morphant, and not mutant (as *llgl1* homozygotes are at times viable) embryos being used? The images shown in panel 3B suggest a fair amount of variability in signal from cell to cell. Quantification of Yap antibody staining may be preferable here.

Author Response: Originally, we had opted to use the *llgl1*^{mw83} line solely for our studies. However, we found that any procedure requiring microinjection resulted in lethality in *llgl1*^{-/-} embryos. Given the strong similarity in phenotypes between *llgl1* mutants and morphants, we opted to use the morphant line for some of our studies due to technical feasibility. We have clarified this in section 3.3 where we first characterize morphant embryos... Considering *llgl1*^{-/-} mutant embryos do not withstand microinjection, potentially due to epidermal adhesion/resealing defects, a previously validated *llgl1* morpholino was used to mediate knockdown of *Llgl1* for subsequent co-injection experiments (Clark et al., 2012). We first assessed cardiac phenotypes of *llgl1* morphant embryos which present a strong similarity in gross morphology to *llgl1*^{-/-} mutants (Fig. S3).

... and emphasized this point in section 3.4 where we introduce exogenous construct expression:

“Interestingly, llgl1^{-/-} embryos were sensitive to microinjection, failing to develop after perturbation at the one-cell stage, thus necessitating the use of the llgl1 morpholino. Exogenous expression of Yap in cardiomyocytes...”

We also now clarify the expression of eGFP-Yap constructs is accomplished with Tol2 transposable vectors (depicted in Figure 7, formerly Figure 3):

*“To visualize Yap localization in the zebrafish epidermis, we expressed eGFP-Yap^{S54A} and eGFP-Yap^{S54A;S335A} under the epidermal *krt18* promoter via the Tol2 transposable constructs.”*

Variability in signal from cell-to-cell in each group is also now acknowledged in Section 3.5:

“Compared to controls, the *llgl1* morphant epidermis lacked membrane localization and, although the eGFP-Yap^{S54A} signal varied from cell-to-cell, the eGFP-Yap^{S54A} signal was significantly decreased in intensity.”

3. To the non-expert, interpretation of the EM images of skin phenotypes is difficult. Some form of schematic in Figure S2 would help in this regards.

Author Response: We agree with the reviewer that electron micrographs can be difficult to interpret. To aid readers we have added a color overlay to Figure S11 (formerly S2) delineating the regions of interest:

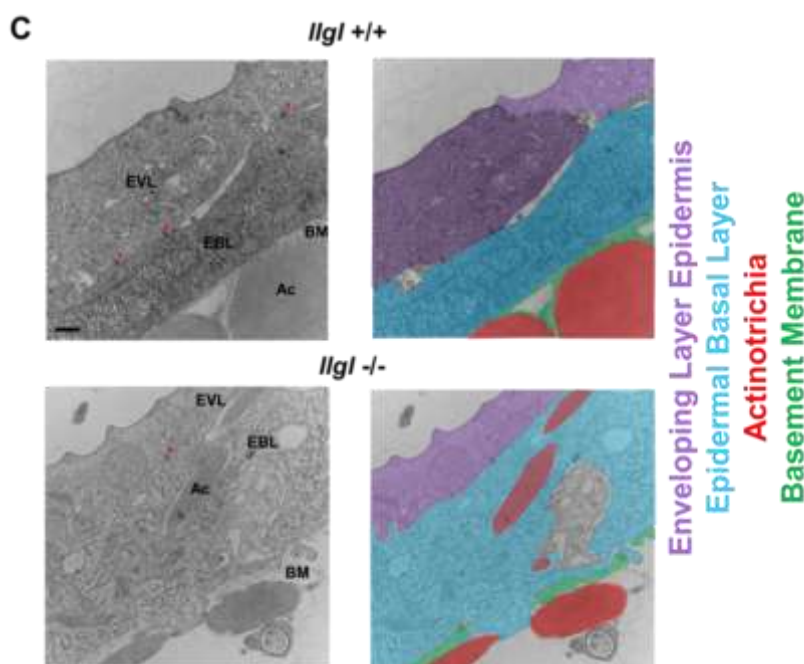


Fig. S11. Loss of *Llgl1* causes epidermal abnormalities in cold raised embryos. (C) Representative electron micrographs depicting fin epidermal layers in 5 dpf staged embryos and pseudocolored schematic depicting various cells and structures. Note the lack of hemidesmosome formation in *llgl1*^{-/-} mutants (red arrow). Enveloping epidermal layer (EVL), epidermal basal layer (EBL), basement membrane (BM), actinotrichia (Ac). Scale = 500 nm.”

4. In lines 358-361, assuming ventricular chamber size from ESV and EDV measures seems like a stretch. These measures are affected by a number of factors, including load/pre-load, contractility, etc.

Author Response: The reviewer makes a valid point. As our adult cardiac assessments are limited to echocardiography, we have revised this passage in Section 3.3 to remove claims of differences in heart size:

“Although approximately 30% of *llgl1*^{-/-} fish die, the remaining fish recover and survive to adulthood. We analyzed three clutches of siblings raised from *llgl1*^{-/-} x *llgl1*^{+/-} crosses by echocardiography to assess cardiac function between genotypes. Echocardiograms revealed variations in cardiac physiology among adult *llgl1*^{-/-} males as indicated by statistically smaller end-diastolic and end-systolic volume (EDV, ESV) measurements when normalized to body length (Fig. 4). Stroke volume was also significantly reduced in males. While no difference was observed in the A wave peak velocity between groups, we observed a significant decrease in maximum E wave velocity in *llgl1*^{-/-} fish as compared to *llgl1*^{+/-} siblings, with no observable differences between sexes of the same genotype. These results illustrated a dysfunction in passive filling of the ventricle during early diastole in *llgl1*^{-/-} fish and a decrease in cardiac function in *llgl1*^{-/-} male fish as compared to *llgl1*^{+/-} male siblings. Together, our observations of *llgl1* mutant and morphant fish illustrates that

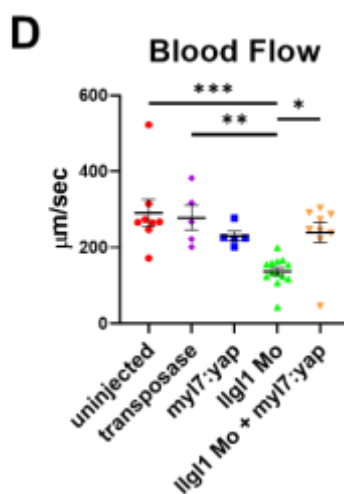
a loss of Llgl1 in zebrafish results in dysmorphic heart development and impaired cardiac function in adult males.”

5. Again in Figure 7, why were morphant embryos used for rescue experiments? The extent of rescue as shown is rather cursory: low numbers and a “pericardial effusion” phenotype. A more robust readout, such as blood toggling or Notch restriction, would be far preferable.

Author Response: As detailed in Reviewer 1’s Question 2, we now explain why *llgl1* morphants were required when utilizing microinjections in the rescue experiments. We agree with the Reviewer that our analysis of pericardial effusion was a superficial assessment of cardiac physiology. To bolster our assessment that exogenous Yap expression in cardiomyocytes ameliorates the abnormal cardiac physiological function associated with loss of *Llgl1*, we tested whether co-injection of our *myl7:Yap-myc* construct in *llgl1* morphants rescued blood flow velocity. We found that, indeed, injection of *myl7:Yap-myc* significantly rescued blood flow velocity in *llgl1* morphants. These results strongly suggest a cardiomyocyte centric role for *Llgl1* in regulating blood flow velocity which we detail in section 3.4...

“Exogenous expression of Yap in cardiomyocytes ameliorated the pericardial effusion phenotype of *llgl1* morphants at 3 dpf (Fig. 6C). Furthermore, analysis of hemodynamic forces showed a statistically significant increase in blood flow velocity with co-injection of the *myl7:Yap-myc* construct in *llgl1* morphants as compared *llgl1* morphants alone (Fig. 6D). No statistical difference in blood flow velocity was observed between in the *myl7:Yap-myc* treated *llgl1* morphants or *myl7:Yap-myc* treated wildtype embryos and the control groups. This amelioration of deleterious cardiac physiology is consistent with the decrease in Yap protein.”

...and the additional data has been included in Figure 6 D.



“Fig. 6. *Llgl1* promotes appropriate Yap protein levels in cardiomyocytes and exogenous expression of Yap in cardiomyocytes ameliorates deleterious cardiac physiology associated with loss of *Llgl1*. (D) Quantification of blood flow velocity in 2 dpf embryos. $n = 8$ uninjected control group, 5 transposase only control group, 5 for *myl7:yap-myc* control group, 13 for *llgl1* morphants, and 9 for *llgl1* morphants with *myl7:yap-myc* expression. One-way ANOVA, Tukey’s multiple comparisons test. * $p < 0.05$, ** $p < 0.01$, *** $p < 0.001$.”

6. The statement on lines 412-413 that “The effect of *Llgl1* on Yap levels, but not cell junction localization, depended on Serine 335 of Yap” is not supported by quantitative data in this study. Junctional localization also appears to be reduced in images shown.

Author Response: We have clarified this statement to illustrate that, while Yap junctional

localization is affected by Llg1, the decrease in Yap itself is ultimately mediated by phosphorylation of Serine 335. Indeed, as the Reviewer states, both instances of junctional localization in *llgl1* morphant embryos appear to show reduced junctional localization of Yap in **Figure 7**. The new passage from Discussion reads as follows:

“Our in vivo data show loss of Llg1 resulted in delocalization of Yap from the membrane in epidermal cells rendering Yap susceptible to degradation. The effect of Llg1 on Yap levels, but not cell junction localization, depended on Serine 335 of Yap- a known target of Lats kinases which prime Yap for degradation.”

7. Given the low penetrance of severe defects in *llgl1* mutants, the title should be modified from “essential” in describing a role for Llg1 in cardiac morphogenesis and valve formation.

Author Response: The Reviewer makes a valid critique. While all *llgl1*^{-/-} embryos displayed pericardial effusion at 3 dpf to some degree of variable expression, the phenotype was transient for a subset of mutants which developed normally. Given the addition of physiological data assessing embryonic function and morphology specifically of cardiomyocytes, the title has been revised to “Llg1 regulates zebrafish cardiac development by mediating Yap stability in cardiomyocytes.”

Reviewer 2

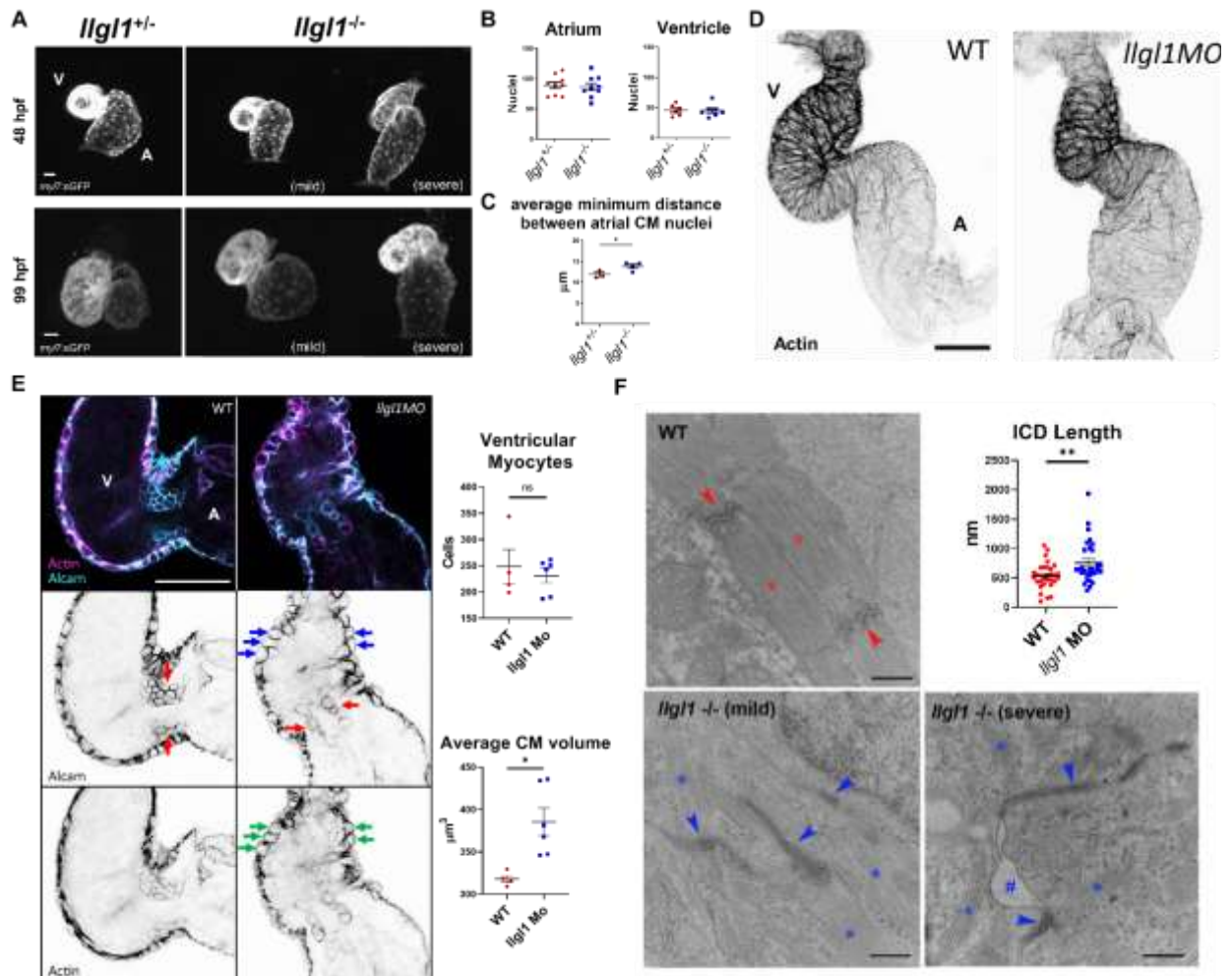
1. It is interesting to observe the pericardial edema in the *llgl1*^{-/-} embryos. However, the phenotypic description is rather simplistic. An extensive and rigorous characterization of gene expression patterns, cardiomyocyte differentiation states, morphology, and cellular morphometrics in the ventricular and atrial chambers would enhance the quality of this manuscript. Furthermore, these new data could offer a more detailed assessment of (and explanation for) the variable expressivity of the *llgl1*^{-/-} phenotype.

Author Response: We agree with the Reviewer and have revised the manuscript to focus on Llg1's role in regulating Yap protein levels in cardiomyocytes and how this affects cardiac morphogenesis and physiology. Specifically, we now perform morphometric analyses on ventricular and atrial cardiomyocytes, finding larger cells in both chambers at 48 hpf with no change in cell number in *llgl1* morphants. Additionally, we performed electron microscopy on 4 dpf *llgl1*^{-/-} mutants and 2 dpf *llgl1* morphant hearts, finding elongated, dysmorphic intercalated discs, as well as a reduction in sarcomere bundles. This additional data is covered in Section 3.3...

*“To assess how the loss of Llg1 affects cardiac development, we crossed the *llgl1*^{mw83} line with a cardiomyocyte-reporter transgenic line *Tg(myl7:eGFP)*^{mw45} to visualize cardiomyocytes during development. At 48 hours post fertilization (hpf), a subset of *llgl1*^{-/-} embryos failed to undergo cardiac looping, whereas *llgl1*^{-/-} embryos with slight pericardial effusion resembled *llgl1*^{+/-} siblings (Fig. 3A). This phenotype was not due to changes in atrial or ventricular cardiomyocyte cell numbers as this did not change between groups (Fig. 3B). However, by 99 hpf, *llgl1*^{-/-} hearts appeared larger than *llgl1*^{+/-} siblings (Fig. 3A). Analysis by Imaris software revealed that a loss of Llg1 resulted in larger atrial cardiomyocytes as indicated by increased internuclear distances, indicative of cardiomyocyte hypertrophy (Fig. 3C). Considering *llgl1*^{-/-} mutant embryos do not withstand microinjection, potentially due to epidermal adhesion/resealing defects, a previously validated *llgl1* morpholino was used to mediate knockdown of Llg1 for subsequent co-injection experiments (Clark et al., 2012). We first assessed cardiac phenotypes of *llgl1* morphant embryos which present a strong similarity in gross morphology to *llgl1*^{-/-} mutants (Fig. S3). Embryos injected with the *llgl1* morpholino were verified to show the pericardial effusion phenotype prior to analysis and varied in severity (Fig. S3). Additionally, as with *llgl1*^{-/-} mutant embryos, *llgl1* morphants failed to undergo cardiac looping at 48 hpf, resulting in dysmorphic ventricles (Figs. 3D, S5). Confocal analysis of 48 hpf *llgl1* morphant hearts revealed larger, rounded ventricular cardiomyocytes with an abnormal distribution of actin (Fig. 3E, S6). Prior to trabeculation, ventricular cardiomyocytes develop dense cortically localized myofibrils on the basal/luminal region of the cell (Reischauer et al., 2014). To test whether this atypical distribution of myofibrils might affect the contractile structures of the heart, we performed transmission*

electron microscopy which revealed disorganized and reduced sarcomere bundles in *llgl1* morphant cardiomyocytes at 48 hpf (Fig S7). Similar phenotypes were observed in *llgl1*^{-/-} mutant embryos at 4 dpf which presented dysgenic sarcomeres and enlarged dysmorphic intercalated discs (Figs. 4F, S7). In embryos with a severe pericardial effusion phenotype, adhesion between cardiomyocytes and surrounding cells was affected. The intercalated disc phenotype is reminiscent to the enlarged and dysmorphic adherens junctions observed in *llgl1* morphant retinal neuroepithelia (Clark et al., 2012). Collectively, these results show *Llgl1* regulates development of cardiomyocyte morphology and contraction in the first few days of life in zebrafish.”

...and demonstrated in Figure 3

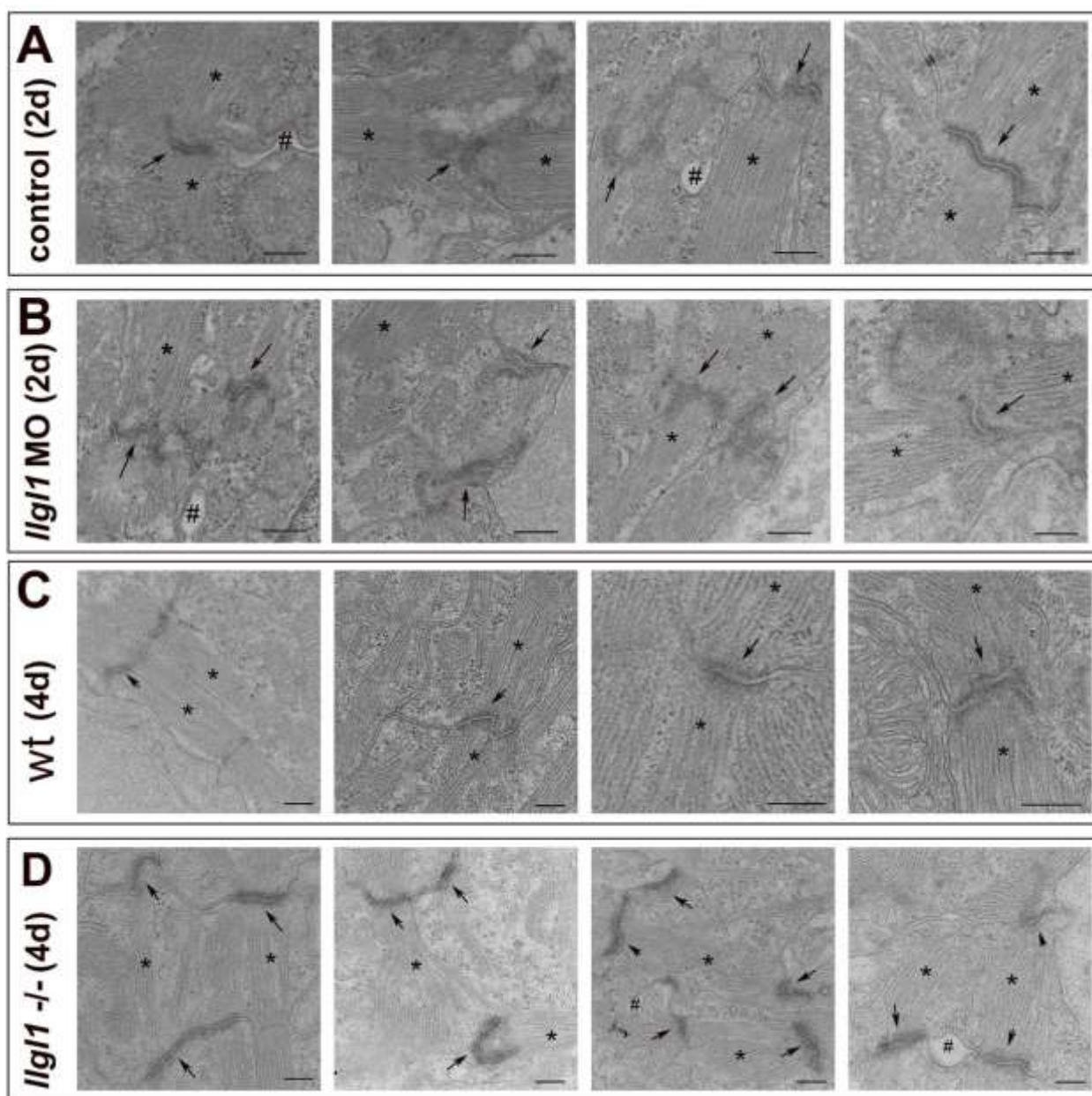


“Fig. 3. Loss of *llgl1* disrupts normal heart development. (A) Representative confocal z-stack images of hearts expression *myl7:eGFP* at 48 and 99 hpf in *llgl1*^{+/-} and *llgl1*^{-/-} siblings. A = atrium, V = ventricle. Scale = 25 μm . (B) Quantification of atrial and ventricular cardiomyocyte nuclei in 48 hpf *llgl1* morphants vs uninjected controls. $n = 9$ for atrial nuclei analysis. $n = 6$ for uninjected control and 7 for *llgl1* morpholino microinjection for ventricular nuclei analysis. Two-tailed unpaired student’s *t*-test. (C) Quantification of average minimum distance between atrial cardiomyocyte nuclei in *llgl1*^{+/-} and *llgl1*^{-/-} siblings at 48 hpf. $n = 3$ *llgl1*^{+/-} hearts and 4 *llgl1*^{-/-} hearts. Two-tailed unpaired student’s *t*-test. (D) Representative confocal z-stack images of actin stain 48 hpf hearts. Scale = 50 μm . (E) Representative single section confocal micrograph of Alcarn or Actin stained 48 hpf hearts, focusing on the AVC. Red arrows depict valve leaflets. Blue arrows depict large, rounded ventricular cardiomyocytes. Green arrows depict abnormal actin staining in myocardium. Scale = 50 μm . Quantification of ventricular cardiomyocyte number and volume. $n = 4$ untreated embryos and 6 *llgl1* morpholino treated embryos Two-tailed unpaired student’s *t*-test. (F) Representative

electron micrographs of 4 dpf wild-type and *llgl1*^{-/-} cardiomyocytes. Red asterisks denote normal sarcomeres of wild-type, while blue asterisks denote thin and disorganized sarcomeres of *llgl1*^{-/-} cardiomyocytes. Red arrows illustrate normal intercalated discs of wild-type, while blue arrows indicate elongated, dysmorphic intercalated discs of *llgl1*^{-/-} cardiomyocytes.

Hashtag indicates loss of adhesion between cardiomyocytes. Scale = 500 nm. Quantification of cardiomyocyte intercalated disc length. *n* = 30 intercalated discs per group compiled from 3 animals per group, and 10 micrographs per animal. ns = not significant, **p*<0.05, ***p*<0.01.”

...and Supplemental Figure S7.

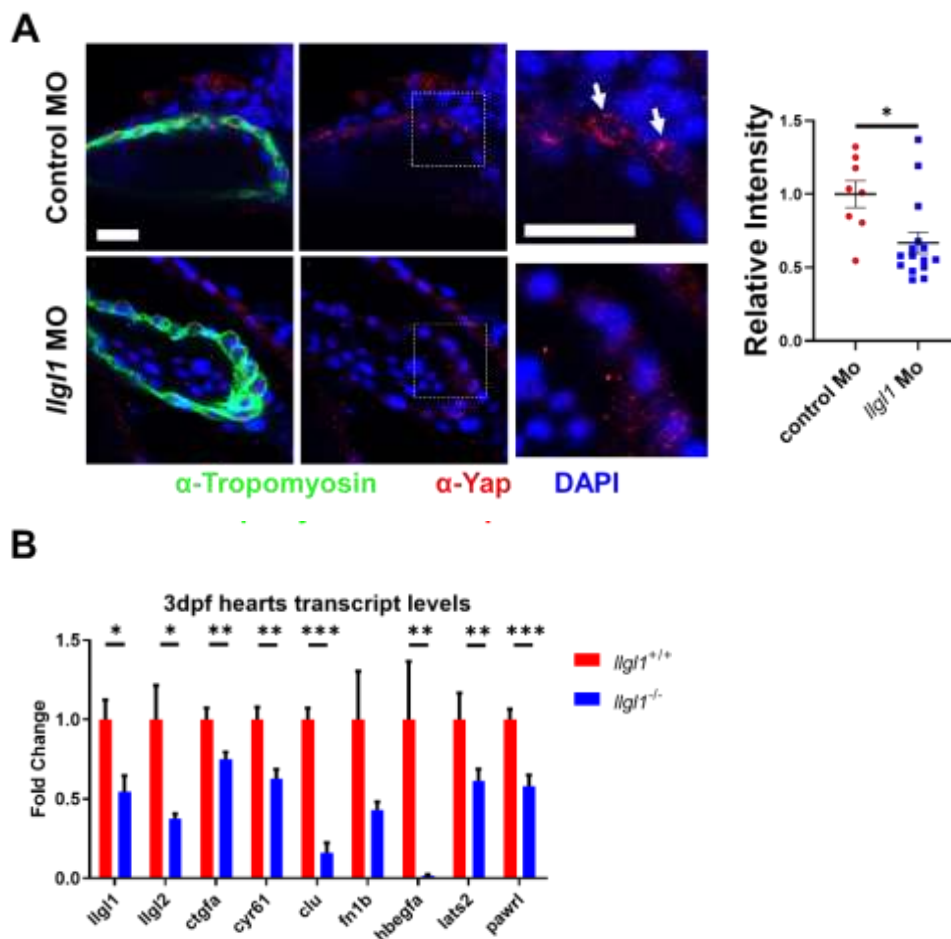


“Fig. S7. Additional images ultrastructural images of 2dpf and 4dpf control and *llgl1* deficient cardiomyocytes. (A) Control and (B) *llgl1* morphant 2 dpf cardiomyocytes. (C) Wild-type and (D) *llgl1*^{-/-} mutant 4 dpf cardiomyocytes. For all images labeling indicates electron dense intercalated discs (arrows), sarcomeres (asterisks), and regions lacking cell adhesion (hashtags). Scale bars = 500 nm.”

Additionally, we performed analyses on Yap protein levels in zebrafish cardiomyocytes *in vivo*, demonstrating a significant decrease in Yap protein in *llgl* morphants at 2 dpf. These data were supplemented with qRT-PCR data for genes associated with Yap activity, which showed a decrease in *llgl1*^{-/-} hearts at 3 dpf. The results of these experiments are now detailed in Section 3.4...

“As we found depletion of *Llgl1* reduced Yap protein levels in rat cardiomyocytes *in-vitro*, we next tested whether, in contrast to *Drosophila*, *in-vivo* depletion of *Llgl1* also reduced Yap protein levels in zebrafish cardiomyocytes. Anti-Yap staining in 2 dpf zebrafish showed a significant decrease of Yap protein signature in the Tropomyosin expressing ventricular cardiomyocytes of *llgl1* morphants compared to controls (Fig. 6A). Ventricles were measured using confocal microscopy and quantified with Imaris software. Furthermore, qRT-PCR analysis revealed a decrease of Yap regulated transcripts from hearts isolated from 3 dpf *llgl1*^{-/-} embryos compared to wildtype (Fig. 6B). Expression of both *llgl1* and *llgl2* transcripts were also significantly decreased. Taken together, this data indicates *Llgl1* regulates Yap protein levels and associated transcriptional activity in zebrafish cardiomyocytes.”

...and illustrated in Figure 6A, B.



“Fig. 6. *Llgl1* promotes appropriate Yap protein levels in cardiomyocytes and exogenous expression of Yap in cardiomyocytes ameliorates deleterious cardiac physiology associated with loss of *Llgl1*. (A) Representative images of 2 dpf zebrafish ventricles from single plane confocal micrographs. Boxes indicate zoomed in area. Arrows depict Yap within cardiomyocytes. Scale = 50 μ m. Quantification of the intensity of anti-Yap signature in Tropomyosin positive cells normalized to the Control morpholino group. $n = 8$ untreated embryos and 15 *llgl1* morpholino treated embryos Two-tailed unpaired student’s *t*-test. (B) qRT-PCR transcript analysis for *llgl1*,

llgl2 and genes regulated by Yap activity in llgl1^{+/+} or llgl1^{-/-} 3 dpf zebrafish hearts. n = 10 for each group. Two-tailed unpaired student's t-test."

2. The authors alternate between use of the llgl1 mutants and morphant embryos, during experiments designed to elucidate Yap protein stability and also those evaluating abnormal cardiac features. If the benefits of one tool or another are preferred due to technical reasons, the rationale should be explicitly stated. Lastly, a more detailed comparison between the llgl1 mutants and morphant phenotypes would be greatly appreciated.

Author Response: Originally, we had opted to use the llgl1^{mw83} line solely for our studies. However, we found that any experiment requiring microinjection resulted in lethality in llgl1^{-/-} embryos. Given the strong similarity in phenotypes between llgl1 mutants and morphants, we opted to use the morphant approach for injection-dependent studies. We have clarified this in section 3.3 where we first characterize morphant embryos...

"Considering llgl1^{-/-} mutant embryos do not withstand microinjection, potentially due to epidermal adhesion/resealing defects, a previously validated llgl1 morpholino was used to mediate knockdown of Llgl1 for subsequent co-injection experiments (Clark et al., 2012). We first assessed cardiac phenotypes of llgl1 morphant embryos which present a strong similarity in gross morphology to llgl1^{-/-} mutants (Fig. S3)."

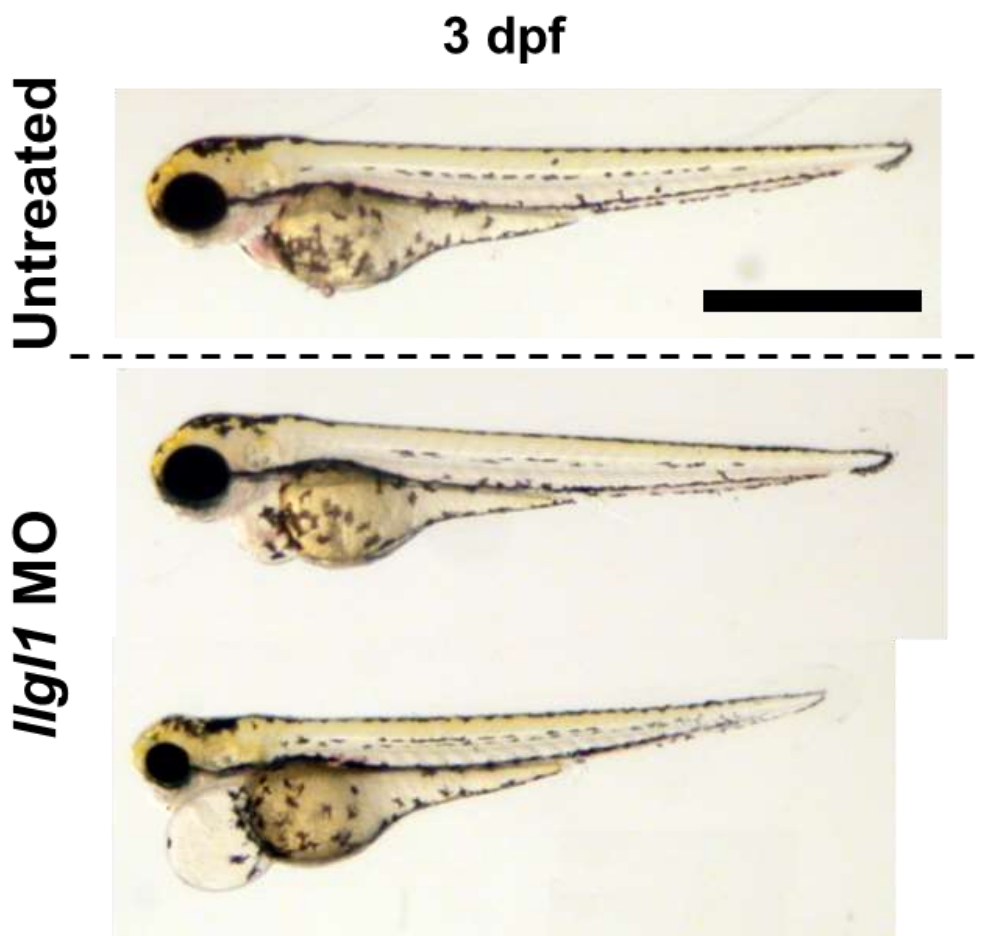
... and emphasized this point in section 3.4 where we introduce exogenous construct expression:

"Interestingly, llgl1^{-/-} embryos were sensitive to microinjection, failing to develop after perturbation at the one-cell stage, thus necessitating the use of the llgl1 morpholino. Exogenous expression of Yap in cardiomyocytes..."

Of relevance, previously published work characterized the variable expressivity of pericardial effusion following morpholino knock-down on Llgl1 (PMID: 22492354) and is now described in Section 3.2...

"Homozygous llgl1 mutant (llgl1^{-/-}) embryos closely resembled the morpholino knock-down phenotype characterize previously in Clark et al., 2012. (Figs. 2B, S3, S4). Pericardial effusion, which can result from cardiac dysfunction, was apparent in all llgl1^{-/-} embryos by 3 days post fertilization (dpf) but varied in expressivity, which was similarly observed in morpholino treated embryos (Figs. 2B, S3)."

Furthermore, we have added an additional Supplemental Figure depicting the variable expressivity of llgl1 morphants:



“Fig. S3. Pericardial effusion in llgl1 morphants. 3 dpf embryos displaying variable expressivity of phenotype. Scale = 1 mm.”

3. Although it is difficult to establish a causative relationship between atrioventricular valve defects and impaired blood flow, it would be extremely helpful if the authors could delineate the temporal dynamics of atrioventricular canal morphogenesis in llgl1^{-/-} embryos. Specifically, are there characteristics of embryonic valve formation that predict functionality at later stages? Moreover, higher quality in situ hybridization images for the probes in Fig. 6D would offer improved assessment of cardiac valve formation.

Author Response: Although the Reviewer brings up an interesting area to explore in regards to characterizing valve formation and development, based on new data, we have revised the manuscript to focus on the effect of Llgl1 in regards to cardiomyocytes. Nonetheless, we do acknowledge the impact of Llgl1 loss on valve development in the Discussion:

“We further identified a novel role for Llgl1 as physiological modifier of zebrafish cardiac development. Phenotypic consequences of Llgl1 disruption on heart morphogenesis included cardiac looping defects, abnormal cardiomyocyte morphology, and atrioventricular valve dysgenesis. Our global Llgl1 depletion model precludes us from determining if abnormal myocardial development subsequently impaired valve development, or if Llgl1 contributes to these developmental processes independently. Evidence from the literature demonstrates that altered hemodynamics can impair valvulogenesis (Donat et al., 2018; Haack and Abdelilah- Seyfried, 2016; Steed et al., 2016). Thus, a primary insult to myocardial contractility and blood flow velocity could secondarily contribute to impaired valvulogenesis and therefore compound hemodynamic-dependent phenotypes through a feed-forward loop. Our data demonstrates that cardiac hemodynamics is at least in part mediated by Llgl1 and Yap activity in cardiomyocytes themselves, as cardiomyocyte specific rescue of Yap in llgl1 morphants restored blood flow velocity to baseline levels. We have yet to determine whether

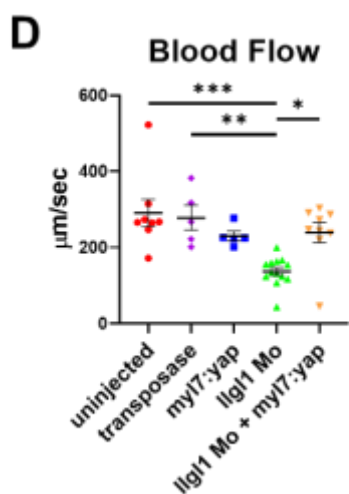
Llgl1 has a direct role in regulating vavulogenesis. However, because *Llgl1* can control of signaling factors such as *Yap* and *Notch*, both which are known to contribute to atrioventricular valve development, this is a possibility. Future studies will address this outstanding question.”

4. Detailed phenotypic investigation (as mentioned in the points above) should be applied to the final experiment in which the requirement for cardiomyocyte-specific *Yap* is determined. Quantification of the degree of pericardial effusion is not an adequate read-out.

Author Response: We agree with the Reviewer that our analysis of pericardial effusion was a cursory assessment of cardiac physiology. To bolster our assessment that exogenous *Yap* expression in cardiomyocytes ameliorates the abnormal cardiac physiological function associated with loss of *Llgl1*, we tested whether co-injection of our *myl7:Yap-myc* construct in *llgl1* morphants rescued blood flow velocity. We found that, indeed, injection of *myl7:Yap-myc* significantly rescued blood flow velocity in *llgl1* morphants. These results strongly suggest a cardiomyocyte centric role for *Llgl1* in regulating blood flow velocity which we detail in section 3.4...

“Exogenous expression of *Yap* in cardiomyocytes ameliorated the pericardial effusion phenotype of *llgl1* morphants at 3 dpf (Fig. 6C). Furthermore, analysis showed a statistically significant increase in blood flow velocity with co-injection of the *myl7:Yap-myc* construct in *llgl1* morphants as compared *llgl1* morphants alone (Fig. 6D). No statistical difference in blood flow velocity was observed between in the *myl7:Yap-myc* treated *llgl1* morphants or *myl7:Yap-myc* treated wildtype embryos and the control groups. This amelioration of deleterious cardiac physiology is consistent with the decrease in *Yap* protein.”

...and the additional data has been included in Figure 6 D:



“Fig. 6. *Llgl1* promotes appropriate *Yap* protein levels in cardiomyocytes and exogenous expression of *Yap* in cardiomyocytes ameliorates deleterious cardiac physiology associated with loss of *Llgl1*. (D) Quantification of blood flow velocity in 2 dpf embryos. $n = 8$ uninjected control group, 5 transposase only control group, 5 for *myl7:yap-myc* control group, 13 for *llgl1* morphants, and 9 for *llgl1* morphants with *myl7:yap-myc* expression. One-way ANOVA, Tukey’s multiple comparisons test. * $p < 0.05$, ** $p < 0.01$, *** $p < 0.001$.”

Minor Points:

1. Panel E is not labeled in Figure 4.

Author Response: The typo has been corrected and should reflect panel D of **Figure 3**, formerly **Figure 4**.

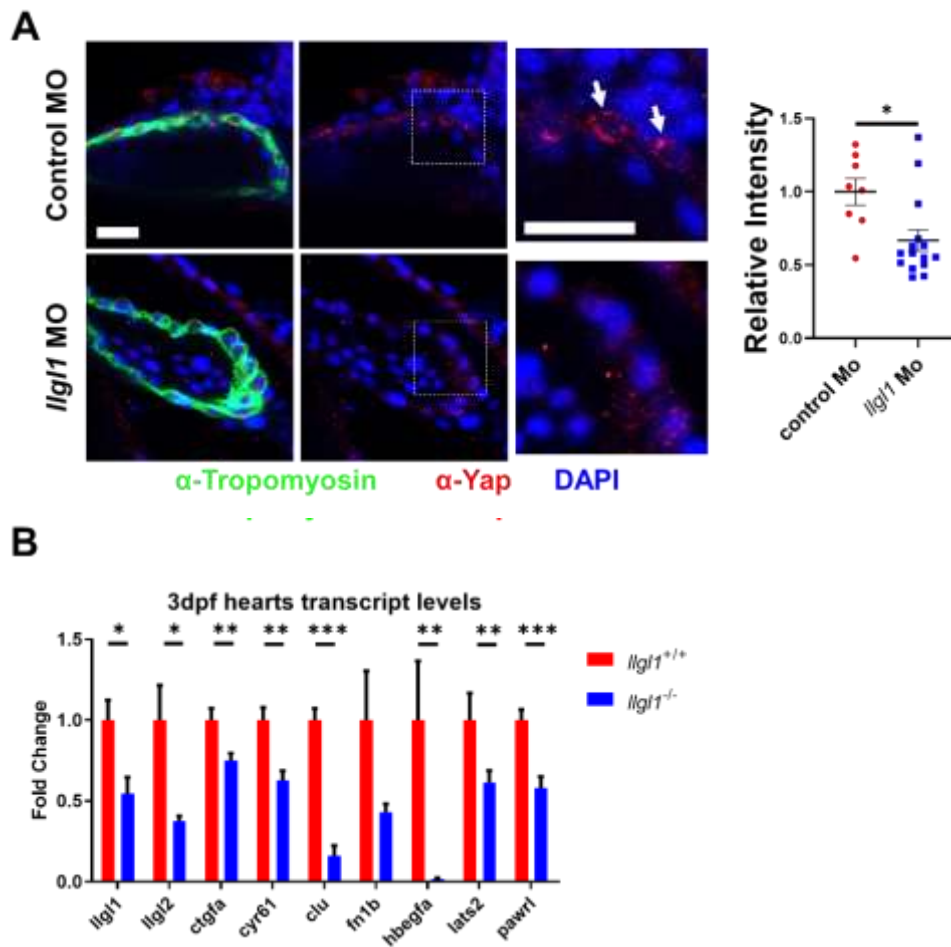
Reviewer 3

1. The authors study the role of *Llgl1* and *Yap* in the heart, but they have not shown expression of either in fish cardiac tissue.

Author Response: The reviewer is correct that cardiac expression of *Llgl1* and *Yap* was lacking. We now include analyses on *Yap* protein levels in zebrafish cardiomyocytes *in vivo*, demonstrating a significant decrease in *Yap* protein in *llgl* morphants at 2 dpf. These data were supplemented with qRT-PCR data for genes associated with *Yap* activity, which showed a decrease in *llgl1*^{-/-} hearts at 3 dpf. These data support the central hypothesis that *Llgl1* is required to maintain appropriate *Yap* protein levels in vertebrate cardiomyocytes and are now detailed in Section 3.4...

*“As we found depletion of *Llgl1* reduced *Yap* protein levels in rat cardiomyocytes in-vitro, we next tested whether, in contrast to *Drosophila*, in-vivo depletion of *Llgl1* also reduced *Yap* protein levels in zebrafish cardiomyocytes. Anti-*Yap* staining in 2 dpf zebrafish showed a significant decrease of *Yap* protein signature in the Tropomyosin expressing ventricular cardiomyocytes of *llgl1* morphants compared to controls (Fig. 6A). Ventricles were measured using confocal microscopy and quantified with Imaris software. Furthermore, qRT-PCR analysis revealed a decrease of *Yap* regulated transcripts from hearts isolated from 3 dpf *llgl1*^{-/-} embryos compared to wildtype (Fig. 6B). Expression of both *llgl1* and *llgl2* transcripts were also significantly decreased. Taken together, this data indicates *Llgl1* regulates *Yap* protein levels and associated transcriptional activity in zebrafish cardiomyocytes.”*

...and illustrated in **Figure 6A, B**.



“Fig. 6. *Lgl1* promotes appropriate *Yap* protein levels in cardiomyocytes and exogenous expression of *Yap* in cardiomyocytes ameliorates deleterious cardiac physiology associated with loss of *Lgl1*. (A) Representative images of 2 dpf zebrafish ventricles from single plane confocal micrographs. Boxes indicate area of enlargement. Arrows depict *Yap* within cardiomyocytes. Scale = 50 μ m. Quantification of the intensity of anti-*Yap* signature in Tropomyosin positive cells normalized to the Control morpholino group. $n = 8$ untreated embryos and 15 *Lgl1* morpholino treated embryos Two-tailed unpaired student’s *t*-test. (B) qRT-PCR transcript analysis for *lgl1*, *lgl2* and genes regulated by *Yap* activity in *lgl1*^{+/+} or *lgl1*^{-/-} 3 dpf zebrafish hearts. $n = 10$ for each group. Two-tailed unpaired student’s *t*-test.”

Additionally, efforts were made to stain for *Lgl1* protein, however we were unable to find a viable antibody for zebrafish. We acknowledge this now in the Discussion:

*“However, as we could not find a *Lgl1* antibody specific for zebrafish, we cannot rule out splicing variants or alternative start sites accounting for some diminished form of *Lgl1* expression in *lgl1*^{mw8} mutant fish. Nonetheless, we show depletion of *Lgl1* in cultured rat cardiomyocytes and zebrafish cardiomyocytes and epidermal cells in vivo resulted in lower levels of total *Yap* protein. Furthermore, depletion of *Lgl1* also resulted in diminished expression of *Yap*-TEAD target genes in both *lgl1*^{-/-} mutant zebrafish and cultured rat cardiomyocytes.”*

2. It would also be nice to see that *Yap* levels are actually downregulated in the heart in the *lgl1* mutant, as this is alluded to but not shown.

Author Response: While we did not assess the *lgl1* mutant line directly for downregulation of *Yap*, we leverage the morpholino extensively in our revision, showing depletion of *Lgl1* results in

decrease Yap protein levels in cardiomyocytes. In conjunction with the *in-vitro* data, the new physiological and immunohistology assessment of *llgl1* morphants (given the strong resemblance to *llgl1*^{-/-} mutant embryos) further support the central hypothesis that Yap protein levels in vertebrate cardiomyocytes are regulated by *Llgl1*.

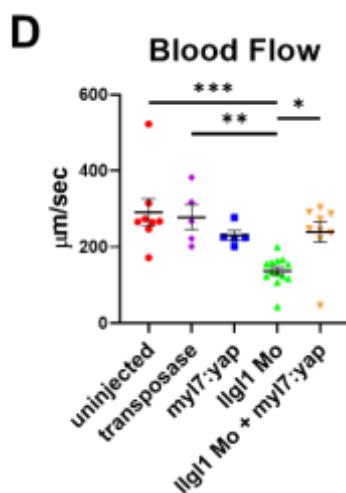
3. Fig. 7 shows that exogenous expression of Yap in the heart alleviates the *llgl1* morphant phenotype, but this data is not convincing (see below) and thus the hypothesis that heart problems in the *llgl1* mutant could be due to changes in Yap dynamics remains unproven.

Author Response: We agree with the Reviewer that our analysis of pericardial effusion was a broad assessment of cardiac physiology. To better address whether exogenous Yap expression in cardiomyocytes ameliorates the abnormal cardiac function associated with loss of *Llgl1*, we tested whether co-injection of our *myl7:Yap-myc* construct in *llgl1* morphants rescued blood flow velocity. We found that, indeed, injection of *myl7:Yap-myc* significantly rescued blood flow velocity in *llgl1* morphants. These results strongly suggest a cardiomyocyte centric role for *Llgl1* in regulating blood flow velocity which we detail in section 3.4...

“Exogenous expression of Yap in cardiomyocytes ameliorated the pericardial effusion phenotype of llgl1 morphants at 3 dpf (Fig. 6C). Furthermore, analysis of hemodynamic forces showed a statistically significant increase in blood flow velocity with co-injection of the myl7:Yap-myc construct in llgl1 morphants as compared llgl1 morphants alone (Fig. 6D). No statistical difference in blood flow velocity was observed between in the myl7:Yap-myc treated llgl1 morphants or

myl7:Yap-myc treated wildtype embryos and the control groups. This amelioration of deleterious cardiac physiology is consistent with the decrease in Yap protein.”

...and the additional data has been included in Figure 6 D:



“Fig. 6. *Llgl1* promotes appropriate Yap protein levels in cardiomyocytes and exogenous expression of Yap in cardiomyocytes ameliorates deleterious cardiac physiology associated with loss of *Llgl1*. (D) Quantification of blood flow velocity in 2 dpf embryos. *n* = 8 uninjected control group, 5 transposase only control group, 5 for *myl7:yap-myc* control group, 13 for *llgl1* morphants, and 9 for *llgl1* morphants with *myl7:yap-myc* expression. One-way ANOVA, Tukey’s multiple comparisons test. **p*<0.05, *p*<0.01, ****p*<0.001.”**

4. *llgl1* mutants and morphants are used interchangeably in the manuscript. However, the morphant heart phenotype and their classes of severity are not shown or characterized. This has been previously published in Clark et al. (Supplemental figures 1 and 2), and the authors should definitely refer to it. It should also be clarified, which phenotype (severity class) was

used for the morphant experiments in the present manuscript. As there is no data on the morphant heart phenotype, one cannot judge the specificity of the MO cardiac phenotype, i.e. was the heart phenotype included in analyzing the rescue by *llgl1* mRNA in Clark et al., Fig. S2?

Author Response: We now clarify in our methods which morpholinos were used throughout the manuscript in Section 2.3:

“The llgl1 ATG (5’-CCGTCTGAACCTAACTTCATCATC-3’) and control (5’-CCTCTTACCTCAGTTACAATTTATA-3’) morpholinos were microinjected as demonstrated in Clark et al., 2012.”

Originally, we had opted to use the *llgl1^{mw83}* line solely for our studies. However, we found that any procedure requiring microinjection resulted in lethality in *llgl1^{-/-}* embryos. Given the strong similarity in phenotypes between *llgl1* mutants and morphants, we opted to use the morphant line for some of our studies due to technical feasibility. We have clarified this in section 3.3 where we first characterize morphant embryos...

“Considering llgl1^{-/-} mutant embryos do not withstand microinjection, potentially due to epidermal adhesion/resealing defects, a previously validated llgl1 morpholino was used to mediate knockdown of Llgl1 for subsequent co-injection experiments (Clark et al., 2012). We first assessed cardiac phenotypes of llgl1 morphant embryos which present a strong similarity in gross morphology to llgl1^{-/-} mutants (Fig. S3).”

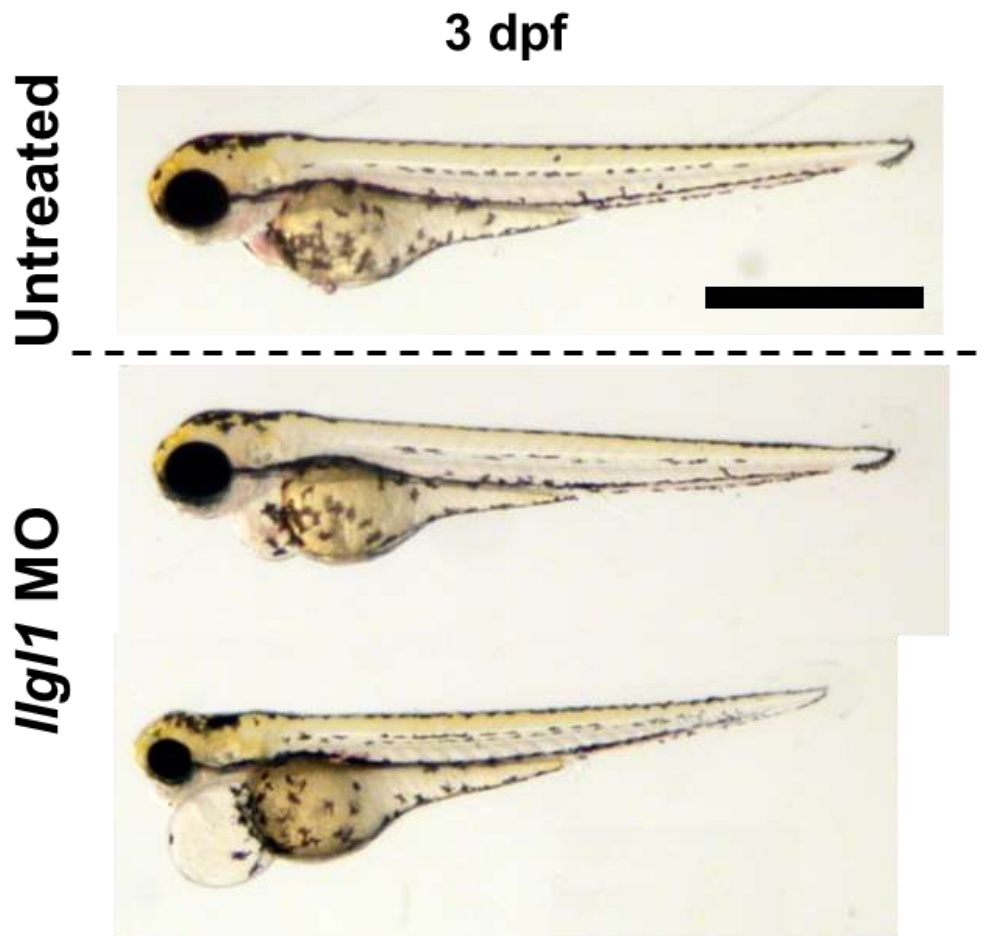
... and emphasized this point in section 3.4 where we introduce exogenous construct expression:

“Interestingly, llgl1^{-/-} embryos were sensitive to microinjection, failing to develop after perturbation at the one-cell stage, thus necessitating the use of the llgl1 morpholino. Exogenous expression of Yap in cardiomyocytes...”

As pointed out by the Reviewer, our previously published work characterized the variable expressivity of pericardial effusion following morpholino knock-down on *Llgl1* (PMID: 22492354) and is now described in Section 3.2...

“Homozygous llgl1 mutant (llgl1^{-/-}) embryos closely resembled the morpholino knock-down phenotype characterize previously in Clark et al., 2012. (Figs. 2B, S3, S4). Pericardial effusion, which can result from cardiac dysfunction, was apparent in all llgl1^{-/-} embryos by 3 days post fertilization (dpf) but varied in expressivity, which was similarly observed in morpholino treated embryos (Figs. 2B, S3).”

Furthermore, we have added an additional Supplemental Figure depicting the variable expressivity of *llgl1* morphants:



“Fig. S3. Pericardial effusion in *lgl1* morphants. 3 dpf embryos displaying variable expressivity of phenotype. Scale = 1 mm.”

General comments:

- please check nomenclature and scale bars

Author Response: We have corrected any errors we found regarding nomenclature or scale bars.

- for readers who are not experts in zebrafish heart development, the respective chapters are not so easy to follow. Highlighting structures, which are mentioned in the text, by arrows in the figures, and/or a cartoon, would be very helpful.

Author Response: Additional markings have been added to figures and supplemental figures to clarify zebrafish anatomy. We have also added a new cartoon model summarizing major findings (Figure 8).

Comments to Materials and Methods (not exhaustive)

- Experiments with the keratin18 promoter (Fig. 4) are not described.

Author Response: The methods have been amended to include information on the krt18 constructs in section 2.3:

“Terminally myc-tagged Yap was inserted downstream of the cardiomyocyte-specific promoter myl7 while eGFP-Yap fusion proteins containing mutations at S54A or S54A;S335A was inserted downstream of the krt18 promoter for expression in epithelia cells.”

-How were fish staged (i.e. according to Kimmel et al. 1995)? This is relevant when it comes to the cold-rearing experiments.

Author Response: We have amended section 3.5 to clarify staging:

“In an attempt to rescue embryos exhibiting severe pericardial effusion, we conducted cold rearing and staged embryos to 5 dpf as described in Kimmel et al., 1995.”

-Line 128: please add TALEN sequences

Author Response: This data is now listed in supplemental table S1:

Table S1. TALEN Sequence

| | |
|-----------------------|--|
| Llgl1 TALEN sequence: | TGACCCTCATCGTGAAAAAATCAAGCAGGATCTGTTTGCATTCAATAAGGTA |
|-----------------------|--|

-Line 131: what is the origin of the Tg(myI7:eGFP) line?

Author Response: The Tg(myI7:eGFP)^{mw45} was originated from Meisfeld et al. 2014 and is now referenced in the methods in section 2.1:

“A transgenic zebrafish line expressing enhanced green fluorescent protein under the myI7 cardiomyocyte specific promoter Tg(myI7:eGFP)^{mw45} was used to visualize cardiomyocytes (Miesfeld and Link, 2014).”

-Line 151: which ones of the MOs used in Clark et al. were used in this study? Please state sequences.

Author Response: We have modified Section 2.3 to include the following:

“The llgl1 ATG (5’-CCGTCTGAACCTAACTTCATCATC-3’) and control (5’-CCTCTTACCTCAGTTACAATTTATA-3’) morpholinos were microinjected as demonstrated in Clark et al., 2012.”

Comments to Results

Figure 1.

- panels B and C are switched in legend

Author Response: This typo has been corrected.

- what is the "Untreated" sample in Fig. 1B?

Author Response: The Untreated group were cells not subjected to the transfection protocol. This has been clarified in Section 2.9 of the Methods:

“Isolated cardiomyocytes were plated in Dulbecco’s modified eagle medium (DMEM, Life Technologies) containing 1 g/L glucose, supplemented with 15% Fetal Bovine Serum (FBS) and penicillin-streptomycin (Life Technologies). After 16 hours, cells were treated to either a simple media change (untreated) or transfected with two different siRNAs designed against the same target gene (to achieve robust knockdown) each at a concentration of 25 nM. siRNAs designed against Yap, Llgl1, Llgl2, a combination of Llgl1 and Llgl2, or negative control siRNA (Table S2) were transfected with mission siRNA transfection reagent (Sigma). Untreated and transfected cells were cultured in DMEM supplemented with 7.5% FBS. Forty-eight hours post transfection cells were collected in Trizol for RNA extraction for qRT-PCR and RNAsequencing, or collected in lysis buffer

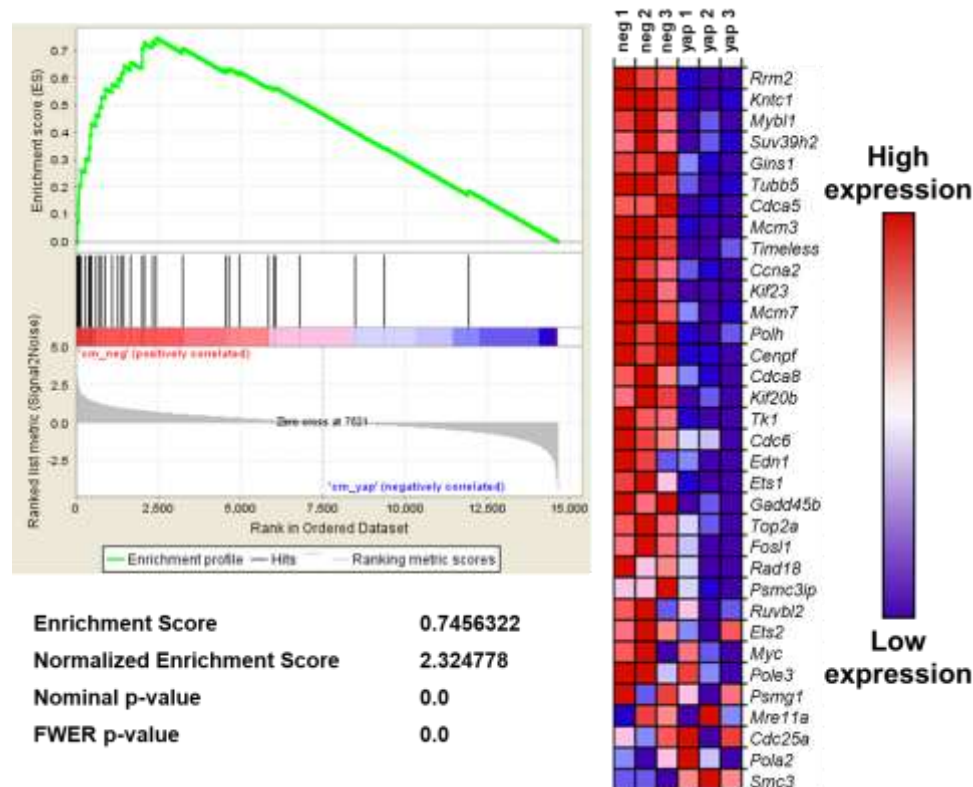
for western blotting as described in O'Meara et al., 2015.”

- Fig. 1C: have these genes shown to be Yap targets in cardiac tissue? This data shows that they are influenced by *Lgl1* loss, but not that this is dependent on Yap. How does this gene set respond to loss of Yap? Was change in expression for any of the targets confirmed by qPCR?

Author Response: To verify the gene set is responsive to loss of Yap, we now show a GSEA on previously generated data from PMID: 30295714. Data is presented in Fig. S1 that depicted significant enrichment of Yap/Wwtr1-Tead target genes in the negative siRNA control compared to cells that have been treated with siRNA against Yap. Section 3.1 has been changed to reflect this...

“This reference gene set was defined by Yap ChIP-Seq and Yap knockdown experiments performed on human MDA-MB-231 cells (Zanconato et al., 2015). We independently verified this GSEA by running the enrichment analysis on RNAseq data generated from cultured rat cardiomyocytes treated with either Yap siRNA or negative control siRNA (Flinn et al., 2019, Fig. S2).”

...and illustrated in Figure S2.



“Fig. S2. Assessment of YAP/WWTR1-TEAD mediated positive regulators of growth upon Yap siRNA knockdown in neonatal rat cardiomyocytes. GSEA for YAP/WWTR1-TEAD target genes involved in proliferation utilizing RNAseq data from cultured rat cardiomyocytes. GSEA was performed on data previously generated in Flinn et al., 2019 and available at GSE112464 of the Gene Expression Omnibus.”

Figure 2.

- what is the penetrance of the cardiac phenotype in *lgl1* morphants? A quantification of the phenotypic classes in morphants is necessary, as morphants are used interchangeably in the manuscript.

Author Response: Only embryos displaying pericardial edema were quantified to ensure delivery

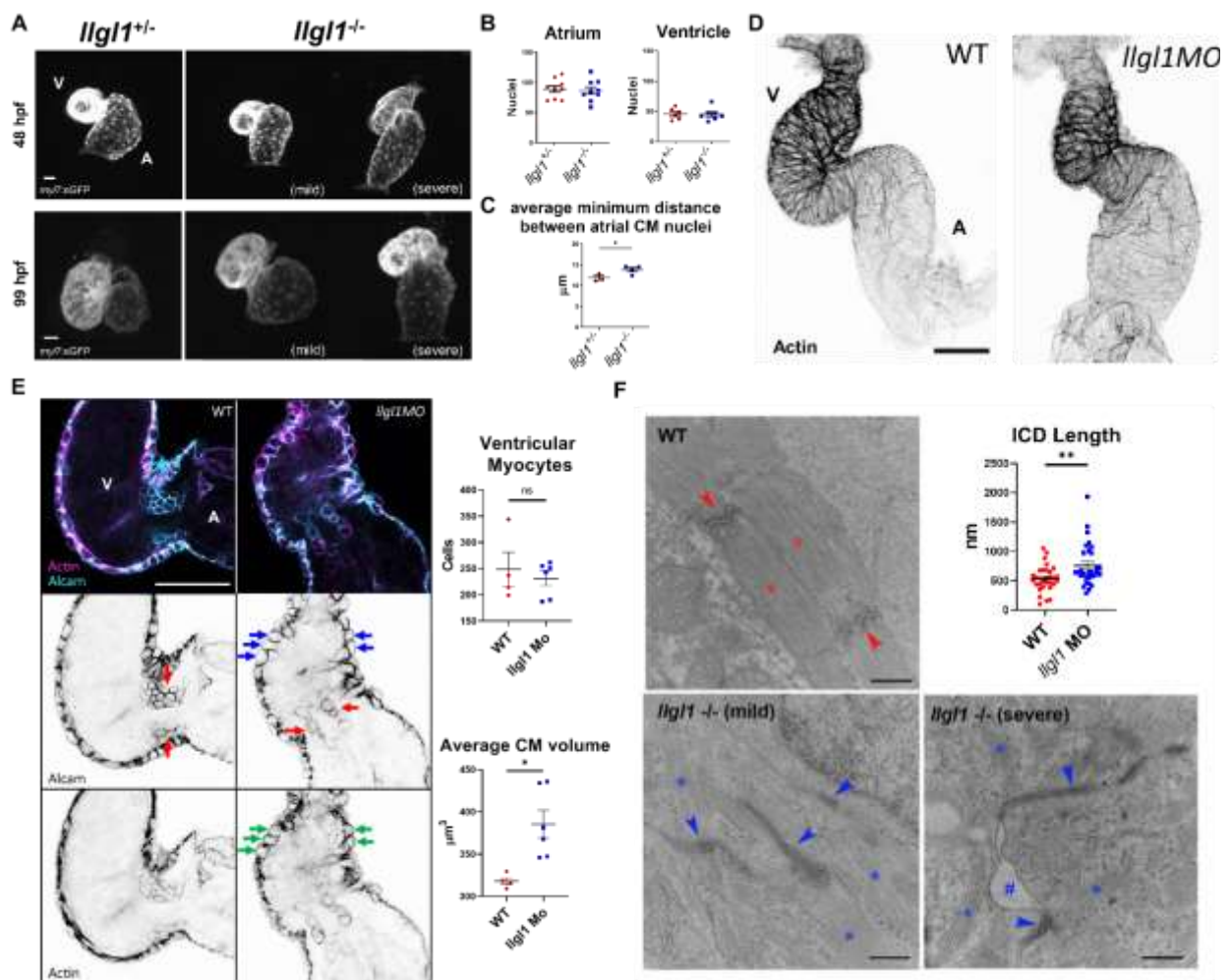
of the morpholino was successful. This is now detailed in section 3.3:

“Embryos injected with the llgl1 morpholino were verified to show the pericardial effusion phenotype prior to analysis and varied in severity (Fig. S3).”

To better assess the cardiac phenotypes between morphant and mutant embryos, we performed morphometrics on 2 dpf morphants and mutants cardiomyocytes and electron microscopy on 4 dpf *llgl1*^{-/-} mutants and 2dpf *llgl1* morphant hearts, finding elongated, dysmorphic intercalated discs. This additional data is covered in Section 3.3...

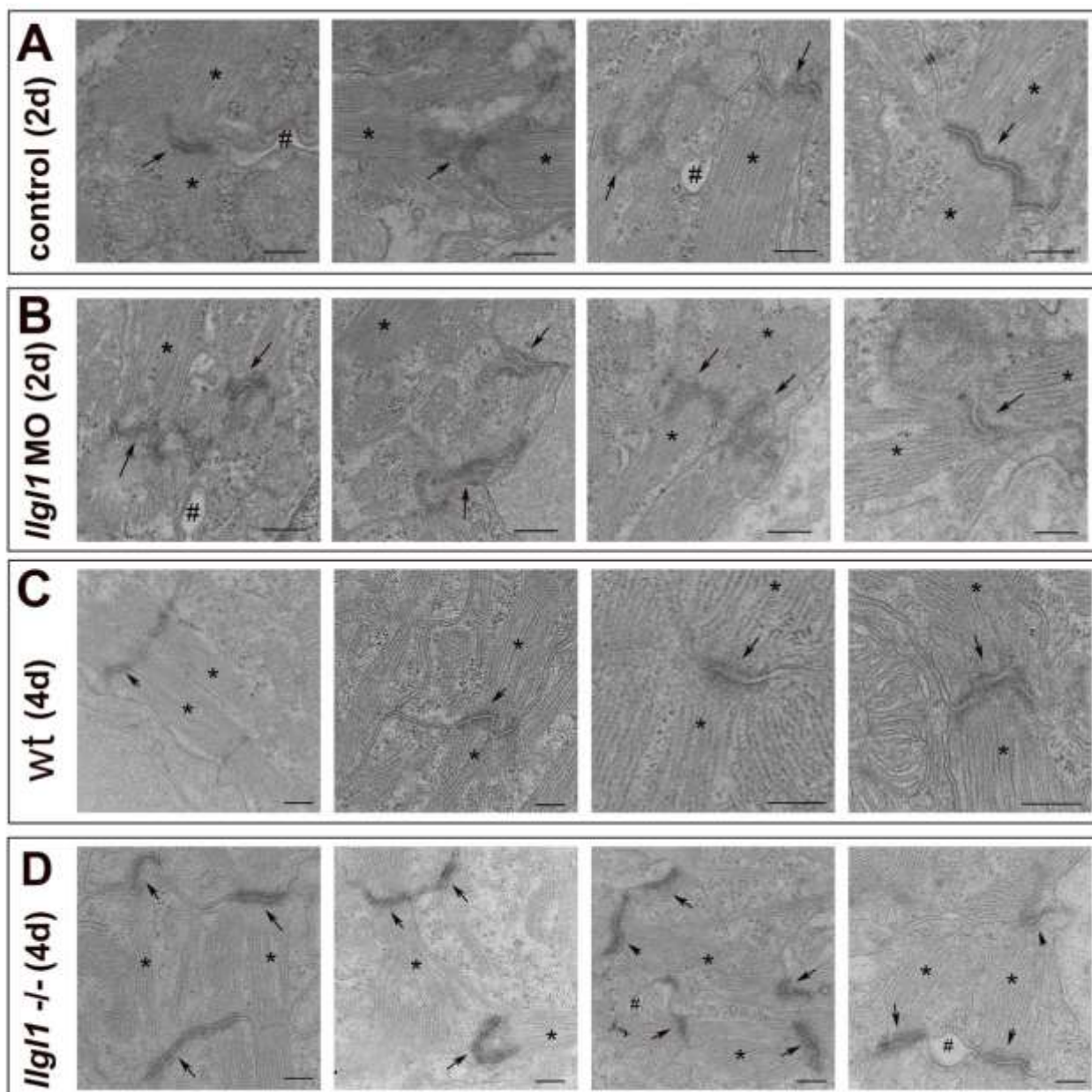
“To assess how the loss of Llgl1 affects cardiac development, we crossed the llgl1^{mw83} line with a cardiomyocyte-reporter transgenic line Tg(myf7:eGFP)^{mw45} to visualize cardiomyocytes during development. At 48 hours post fertilization (hpf), a subset of llgl1^{-/-} embryos failed to undergo cardiac looping, whereas llgl1^{-/-} embryos with slight pericardial effusion resembled llgl1^{+/-} siblings (Fig. 3A). This phenotype was not due to changes in atrial or ventricular cardiomyocyte cell numbers as this did not change between groups (Fig. 3B). However, by 99 hpf, llgl1^{-/-} hearts appeared larger than llgl1^{+/-} siblings (Fig. 3A). Analysis by Imaris software revealed that a loss of Llgl1 resulted in larger atrial cardiomyocytes as indicated by increased internuclear distances, indicative of cardiomyocyte hypertrophy (Fig. 3C). Considering llgl1^{-/-} mutant embryos do not withstand microinjection, potentially due to epidermal adhesion/resealing defects, a previously validated llgl1 morpholino was used to mediate knockdown of Llgl1 for subsequent co-injection experiments (Clark et al., 2012). We first assessed cardiac phenotypes of llgl1 morphant embryos which present a strong similarity in gross morphology to llgl1^{-/-} mutants (Fig. S3). Embryos injected with the llgl1 morpholino were verified to show the pericardial effusion phenotype prior to analysis and varied in severity (Fig. S3). Additionally, as with llgl1^{-/-} mutant embryos, llgl1 morphants failed to undergo cardiac looping at 48 hpf, resulting in dysmorphic ventricles (Figs. 3D, S5). Confocal analysis of 48 hpf llgl1 morphant hearts revealed larger, rounded ventricular cardiomyocytes with an abnormal distribution of actin (Fig. 3E, S6). Prior to trabeculation, ventricular cardiomyocytes develop dense cortically localized myofibrils on the basal/luminal region of the cell (Reischauer et al., 2014). To test whether this atypical distribution of myofibrils might affect the contractile structures of the heart, we performed transmission electron microscopy which revealed disorganized and reduced sarcomere bundles in llgl1 morphant cardiomyocytes at 48 hpf (Fig S7). Similar phenotypes were observed in llgl1^{-/-} mutant embryos at 4 dpf which presented dysgenic sarcomeres and enlarged dysmorphic intercalated discs (Figs. 4F, S7). In embryos with a severe pericardial effusion phenotype, adhesion between cardiomyocytes and surrounding cells was affected. The intercalated disc phenotype is reminiscent to the enlarged and dysmorphic adherens junctions observed in llgl1 morphant retinal neuroepithelia (Clark et al., 2012). Collectively, these results show Llgl1 regulates development of cardiomyocyte morphology and contraction in the first few days of life in zebrafish.”

...and demonstrated in Figure 3



“Fig. 3. Loss of *llgl1* disrupts normal heart development. (A) Representative confocal z-stack images of hearts expression *myl7:eGFP* at 48 and 99 hpf in *llgl1*^{+/-} and *llgl1*^{-/-} siblings. A = atrium, V = ventricle. Scale = 25 μ m. (B) Quantification of atrial and ventricular cardiomyocyte nuclei in 48 hpf *llgl1* morphants vs uninjected controls. $n = 9$ for atrial nuclei analysis. $n = 6$ for uninjected control and 7 for *llgl1* morpholino microinjection for ventricular nuclei analysis. Two-tailed unpaired student’s *t*-test. (C) Quantification of average minimum distance between atrial cardiomyocyte nuclei in *llgl1*^{+/-} and *llgl1*^{-/-} siblings at 48 hpf. $n = 3$ *llgl1*^{+/-} hearts and 4 *llgl1*^{-/-} hearts. Two-tailed unpaired student’s *t*-test. (D) Representative confocal z-stack images of actin stain 48 hpf hearts. Scale = 50 μ m. (E) Representative single section confocal micrograph of Alcain or Actin stained 48 hpf hearts, focusing on the AVC. Red arrows depict valve leaflets. Blue arrows depict large, rounded ventricular cardiomyocytes. Green arrows depict abnormal actin staining in myocardium. Scale = 50 μ m. Quantification of ventricular cardiomyocyte number and volume. $n = 4$ untreated embryos and 6 *llgl1* morpholino treated embryos Two-tailed unpaired student’s *t*-test. (F) Representative electron micrographs of 4 dpf wild-type and *llgl1*^{-/-} cardiomyocytes. Red asterisks denote normal sarcomeres of wild-type, while blue asterisks denote thin and disorganized sarcomeres of *llgl1*^{-/-} cardiomyocytes. Red arrows illustrate normal intercalated discs of wild-type, while blue arrows indicate elongated, dysmorphic intercalated discs of *llgl1*^{-/-} cardiomyocytes. Hashtag indicates loss of adhesion between cardiomyocytes. Scale = 500 nm. Quantification of cardiomyocyte intercalated disc length. $n = 30$ intercalated discs per group compiled from 3 animals per group, and 10 micrographs per animal. *ns* = not significant, * $p < 0.05$, ** $p < 0.01$.”

...and Supplemental Figure S7.



“Fig. S7. Additional images ultrastructural images of 2dpf and 4dpf control and *llgl1* deficient cardiomyocytes. (A) Control and (B) *llgl1* morphant 2 dpf cardiomyocytes. (C) Wild- type and (D) *llgl1*^{-/-} mutant 4 dpf cardiomyocytes. For all images labeling indicates electron dense intercalated discs (arrows), sarcomeres (asterisks), and regions lacking cell adhesion (hashtags). Scale bars = 500 nm.”

- which phenotypic class (mutant and morphant) was used for the analysis?

Author Response: Only mutants were used in Figure 2 and Section 3.2 has been updated to reflect this in their respective titles:

“3.2 Generation of *llgl1* mutant zebrafish”

“Fig. 2. Assessment of *llgl1* mutant gross morphology.”

- Fig. 2B: “hearts fail to undergo chamber ballooning” - can this be labelled in the figure?

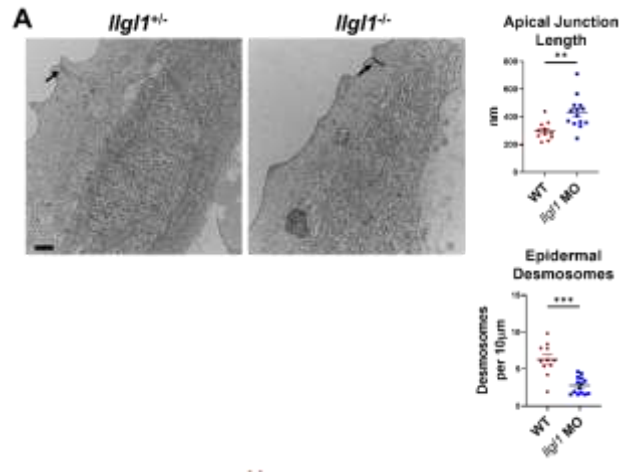
Author Response: We have amended the figure legend to now state:

“Class 3 (severe) - pronounced pericardial effusion and/or body edema, small eyes, hearts fail to undergo cardiac looping (see Supplementary Video S5). “

Figure 3.

- Fig. S2C, decreased density of desmosomes: how many cells were analyzed?
- Fig. 3A: the length of the apical junction was not quantified. Different lengths can also be due to different levels of the sections.

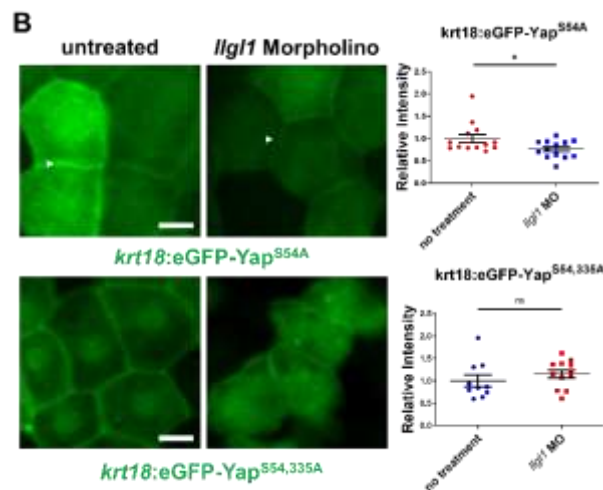
Author Response: We now provide metrics in Figure 7A (formerly Figure 3) to address these concerns:



“Fig. 7. Loss of *Llg1* in zebrafish epidermis results in dysmorphic junctions and increased Yap phospho-degradation. (A) Representative transmission electron micrographs of fin epidermis from 5 dpf stage cold reared embryos. Arrows indicated apical junctions. Scale = 500 nm. Quantification of apical junction length of the outer epidermal layer and the abundance of desmosomes between the epidermal layers. $n = 11 llg1^{+/-}$ and $14 llg1^{-/-}$ embryos. Two-tailed unpaired student's *t*-test.”

- Fig. 3B: what exactly is quantified in the graphs? Intensity per cell or an area of cells? Loss of membrane localization upon *Llg1* KD is not convincing. Quantification of the signal at the membrane vs cytoplasmic signal would help. Scale bar missing.

Author Response: We have clarified the Figure 7B, normalizing the pixel intensity data to the untreated control...



...and the legend to state:

“Quantification of the intensity of the transgene’s signal in positively expression cells is depicted in graphs.”

Furthermore, Section 2.5 has been amended to detail pixel intensity as a metric:

“Resulting images were analyzed using Fiji ImageJ for signal intensity of compiled z-stack images or Imaris for nearest neighbor nuclear distance, cell number, cell size, and pixel intensity for transgene or antibody expression.”

- Yap levels are clearly downregulated (Fig. 3C; scale bar missing), but mislocalization (line 339 “subcellular displacement”?) is not convincing. The premise that Llg1 regulates Yap stability depends on Fig. 3B, which shows a lack of change in Yap^{S54}, 335A levels upon Llg1 KD. No change in Yap levels does not prove that Llg1 regulates phosphodegradation.

Author Response: We now demonstrate that the change in Yap levels is dependent on the accessibility of Serine 335 for phosphorylation, a well characterized target for Lats kinase activity which results in degradation. However, the Reviewer is correct that we do not show Lats is necessary for this event. To clarify, we now state such in section 3.5...

“Expression of plasmid DNA revealed that eGFP-Yap^{S54A} localized to epidermal cell membranes in 30 hpf control embryos (Fig. 7B). Compared to controls, the llgl1 morphant epidermis lacked membrane localization and, although the eGFP-Yap^{S54A} signal varied from cell-to-cell, the eGFP-Yap^{S54A} signal was significantly decreased in intensity. In contrast, expression of the eGFP-Yap^{S54A;S335A} variant, which is resistant to phospho-degradation, showed no change in abundance when compared to control embryos but was also delocalization from the cell cortex. Similarly, an antibody that recognizes Yap revealed a subcellular displacement and reduction in expression levels in 48 hpf llgl1^{-/-} mutants (Figs 7C, S10). Collectively, our results suggest loss of Llg1 affects Yap localization and consequently turnover, potentially through remodeling of apical junctions in epithelia and intercalated discs of cardiomyocytes (Fig. 8). We suspect the loss of Yap protein associated with depletion of Llg1 is ultimately the result of Lats kinase activity.”

Figure 4.

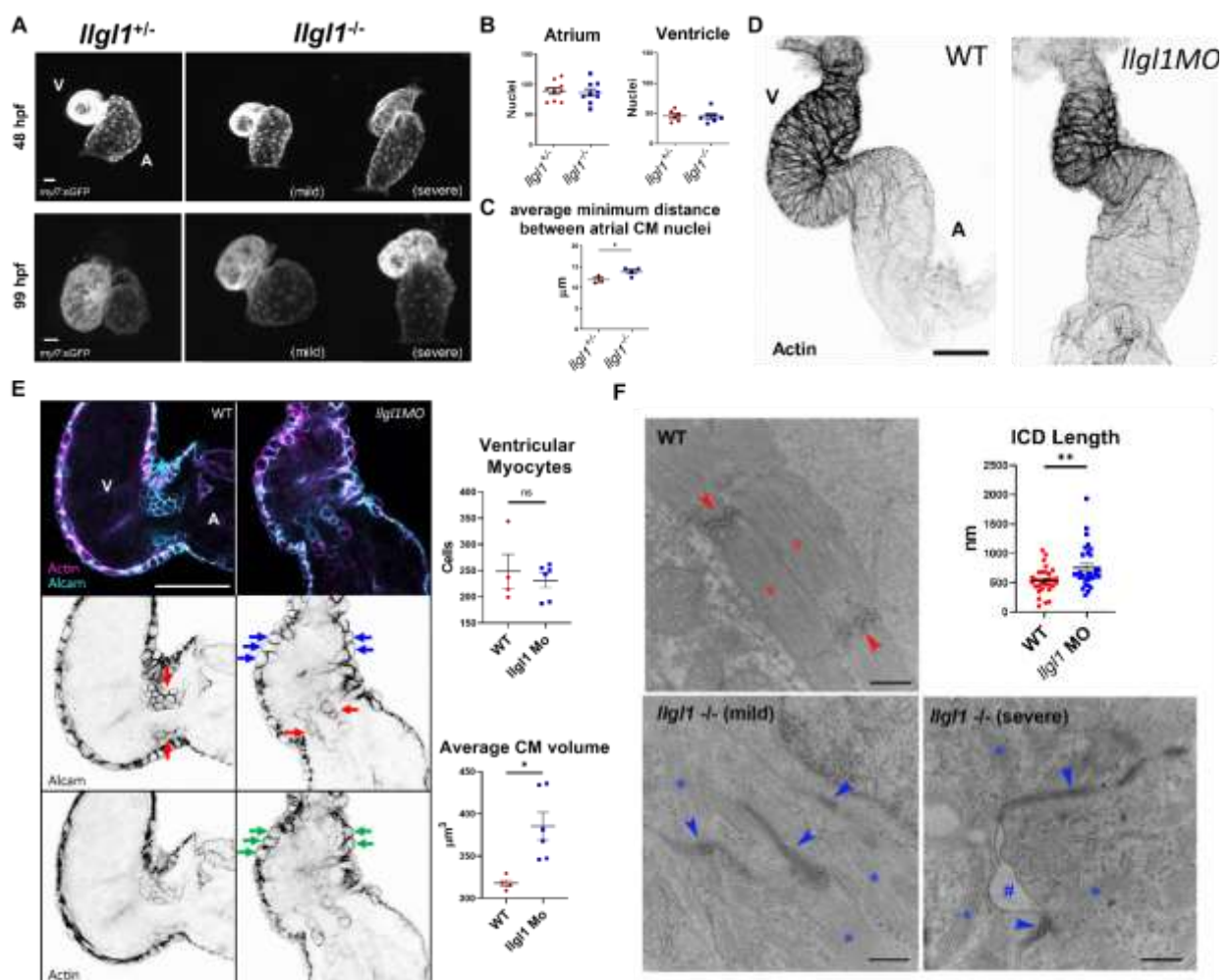
- as above, MO KD is used. It would be important to know the range of cardiac phenotypes caused by Llg1 KD

Author Response: To better assess the cardiac phenotypes between morphant and mutant embryos, we performed morphometrics on 2 dpf morphants and mutants cardiomyocytes and electron microscopy on 4 dpf llgl1^{-/-} mutants and 2dpf llgl1 morphant hearts, finding elongated, dysmorphic intercalated discs. This additional data is covered in Section 3.3...

To assess how the loss of Llg1 affects cardiac development, we crossed the llgl1^{mw83} line with a cardiomyocyte-reporter transgenic line Tg(myf7:eGFP)^{mw45} to visualize cardiomyocytes during development. At 48 hours post fertilization (hpf), a subset of llgl1^{-/-} embryos failed to undergo cardiac looping, whereas llgl1^{-/-} embryos with slight pericardial effusion resembled llgl1^{+/-} siblings (Fig. 3A). This phenotype was not due to changes in atrial or ventricular cardiomyocyte cell numbers as this did not change between groups (Fig. 3B). However, by 99 hpf, llgl1^{-/-} hearts appeared larger than llgl1^{+/-} siblings (Fig. 3A). Analysis by Imaris software revealed that a loss of Llg1 resulted in larger atrial cardiomyocytes as indicated by increased internuclear distances, indicative of cardiomyocyte hypertrophy (Fig. 3C). Given llgl1^{-/-} mutant embryos do not withstand microinjection, use of llgl1 morpholino mediate knockdown of Llg1 was necessary for testing upcoming co-injection experiments. We therefore characterized the cardiac phenotypes of llgl1 morphant embryos which present a strong similarity in gross morphology to llgl1^{-/-} mutants (Fig. S3). Embryos injected with the llgl1 morpholino were verified to show the pericardial effusion phenotype prior to analysis and varied in severity (Fig. S3). Additionally, as with llgl1^{-/-} mutant

embryos, *llgl1* morphants failed to undergo cardiac looping at 48 hpf, resulting in dysmorphic ventricles (Figs. 3D, S5). Confocal analysis of 48 hpf *llgl1* morphant hearts revealed larger, rounded ventricular cardiomyocytes with abnormal distribution of actin (Fig. 3E, S6). Prior to trabeculation, ventricular cardiomyocytes develop dense cortically localized myofibrils on the basal/luminal region of the cell (Reischauer et al., 2014). We suspect this atypical distribution of myofibrils reduces contractile function of the heart. In support of muscle contractile dysfunction, transmission electron microscopy revealed disorganized and reduced sarcomere bundles in *llgl1* morphant cardiomyocytes at 48 hpf (Fig S7). Similar phenotypes were observed in *llgl1*^{-/-} mutant embryos at 4 dpf which presented dysgenic sarcomeres and enlarged dysmorphic intercalated discs (Figs. 4F, S7). In embryos with a severe pericardial effusion phenotype, adhesion between cardiomyocytes and surrounding cells was affected. The intercalated disc phenotype is reminiscent to the enlarged and dysmorphic adherens junctions observed in *llgl1* morphant retinal neuroepithelia (Clark et al., 2012). Collectively, these results show *Llgl1* regulates development of cardiomyocytes in the first few days of life in zebrafish.”

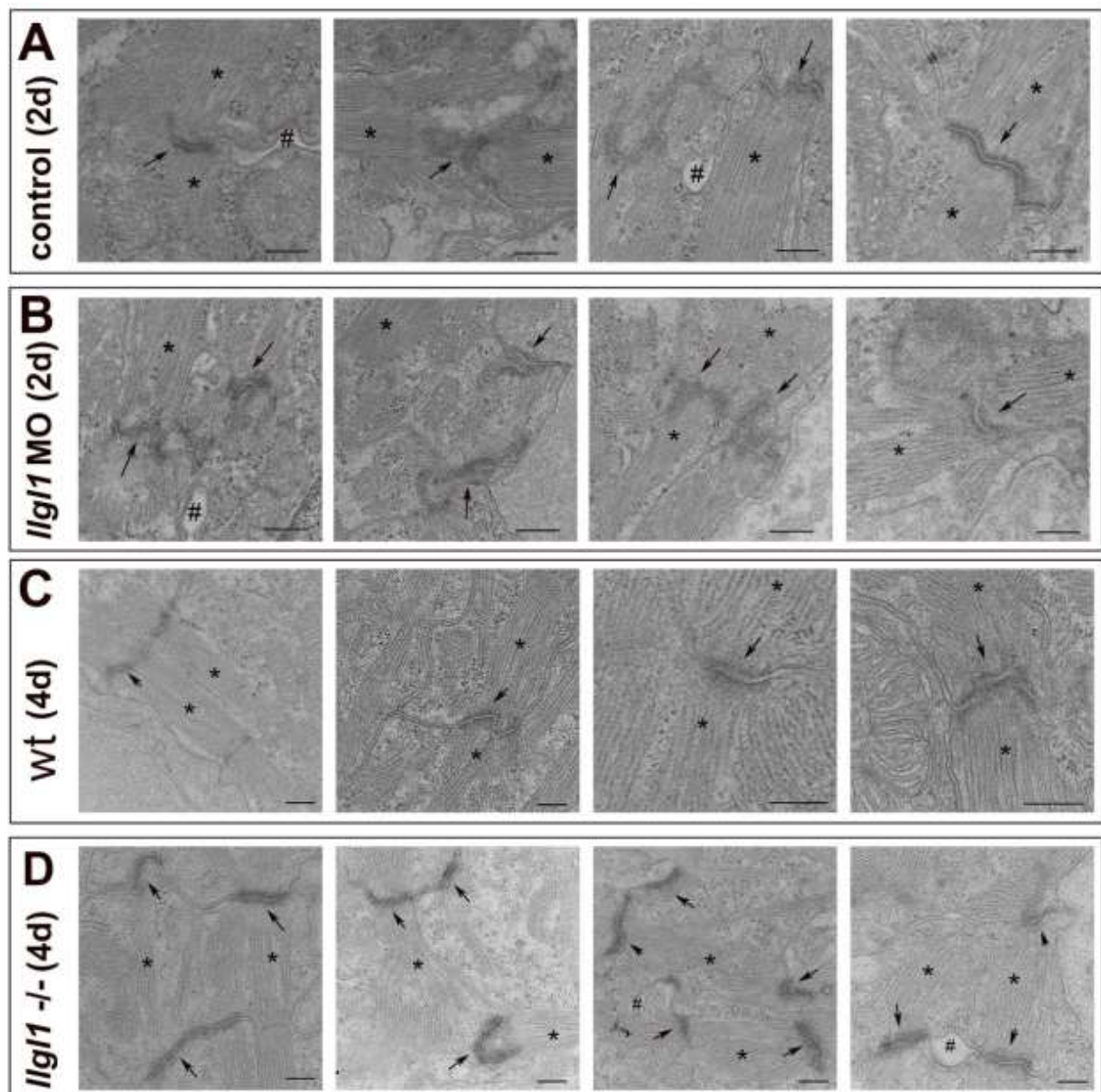
...and demonstrated in Figure 3



“Fig. 3. Loss of *llgl1* disrupts normal heart development. (A) Representative confocal z-stack images of hearts expression *myl7:eGFP* at 48 and 99 hpf in *llgl1*^{+/+} and *llgl1*^{-/-} siblings. A = atrium, V = ventricle. Scale = 25 μm . (B) Quantification of atrial and ventricular cardiomyocyte nuclei in 48 hpf *llgl1* morphants vs uninjected controls. $n = 9$ for atrial nuclei analysis. $n = 6$ for uninjected control and 7 for *llgl1* morpholino microinjection for ventricular nuclei analysis. Two-tailed unpaired student’s *t*-test. (C) Quantification of average minimum distance between atrial cardiomyocyte nuclei in *llgl1*^{+/+} and *llgl1*^{-/-} siblings at 48 hpf. $n = 3$ *llgl1*^{+/+} hearts and 4 *llgl1*^{-/-} hearts. Two-tailed unpaired student’s *t*-test. (D) Representative confocal z-stack images of actin stain 48 hpf hearts. Scale = 50 μm . (E) Representative single section confocal micrograph of Alcain or Actin stained 48

*hpf hearts, focusing on the AVC. Red arrows depict valve leaflets. Blue arrows depict large, rounded ventricular cardiomyocytes. Green arrows depict abnormal actin staining in myocardium. Scale = 50 μ m. Quantification of ventricular cardiomyocyte number and volume. $n = 4$ untreated embryos and 6 *llgl1* morpholino treated embryos Two-tailed unpaired student's *t*-test. (F) Representative electron micrographs of 4 dpf wild-type and *llgl1*^{-/-} cardiomyocytes. Red asterisks denote normal sarcomeres of wild-type, while blue asterisks denote thin and disorganized sarcomeres of *llgl1*^{-/-} cardiomyocytes. Red arrows illustrate normal intercalated discs of wild-type, while blue arrows indicate elongated, dysmorphic intercalated discs of *llgl1*^{-/-} cardiomyocytes. Hashtag indicates loss of adhesion between cardiomyocytes. Scale = 500 nm. Quantification of cardiomyocyte intercalated disc length. $n = 30$ intercalated discs per group compiled from 3 animals per group, and 10 micrographs per animal. ns = not significant, * $p < 0.05$, ** $p < 0.01$.”*

...and Supplemental Figure S7.



“Fig. S7. Additional images ultrastructural images of 2dpf and 4dpf control and *llgl1* deficient cardiomyocytes. (A) Control and (B) *llgl1* morphant 2 dpf cardiomyocytes. (C) Wild-type and (D) *llgl1*^{-/-} mutant 4 dpf cardiomyocytes. For all images labeling indicates electron dense intercalated discs (arrows), sarcomeres (asterisks), and regions lacking cell adhesion (hashtags). Scale bars = 500

nm.”

- labelling atrium and ventricle in the images would be helpful, also referring to either structure in the text in cases where the observations concern one or the other

Author Response: The Figure has been updated to denote the atria and ventricles.

- line 348 "impaired cardiac morphogenesis" - what does this mean? Please define.

Author Response: To clarify, section 3.3 has been amended to now state:
“At 48 hours post fertilization (hpf), a subset of $llgl1^{-/-}$ embryos failed to undergo cardiac looping, whereas $llgl1^{-/-}$ embryos with slight pericardial effusion resembled $llgl1^{+/-}$ siblings (Fig. 3A).”

- line 354-5: "morphants failed to undergo chamber expansion" refers to 4D, not 4E?

Author Response: This has been corrected:
“Additionally, as with $llgl1^{-/-}$ mutant embryos, $llgl1$ morphants failed to undergo cardiac looping at 48 hpf, resulting in dysmorphic ventricles (Figs. 3D, S5).”

Figure 5.

- line 365: not enough individuals analyzed to claim that males have a shortened body axis.

Author Response: This statement has been revised:

“These results illustrated a dysfunction in passive filling of the ventricle during early diastole in $llgl1^{-/-}$ fish and a decrease in cardiac function in $llgl1^{-/-}$ male fish as compared to $llgl1^{+/-}$ male siblings.”

Figure 6.

- panels A, D: scale bar is missing

Author Response: Scale bars have been added to necessary panels.

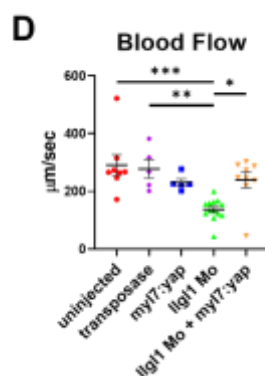
- panel C: y-axis shows percentage of what (whole heart?)

Author Response: The legend has been written to clarify: *“Area of cardiac GFP expression is depicted in the graph.”*

Figure 7.

Numbers of individuals analyzed in this experiment are very low, thus the data is not convincing. What are the cardiac phenotypic classes caused by $llgl1$ MO injection, and how do they change upon the injection of $myl7:Yap-Myc$? What is the efficiency of $Yap-myc$ expression (is it possible to stain for transgene expression), and does that relate to cardiac phenotype? And finally, at what stage were the larvae analyzed?

Author Response: To address the Reviewer’s concerns, we additionally tested the effect exogenous Yap expression in cardiomyocytes had on hemodynamic force by analyzing blood flow velocity in $llgl1$ morphants. Comparing to $llgl1$ morphants groups, $llgl1$ morphants with exogenous Yap expression showed a rescue in blood flow velocity that undistinguishable from either wildtype embryos or the control groups. The additional data has been included in Figure 6D:



“Fig. 6. Llgl1 promotes appropriate Yap protein levels in cardiomyocytes and exogenous expression of Yap in cardiomyocytes ameliorates deleterious cardiac physiology associated with loss of Llgl1. (A) Representative images of 2 dpf zebrafish ventricles from single plane confocal micrographs. Boxes indicate zoomed in area. Arrows depict Yap within cardiomyocytes. Scale = 50 μm. Quantification of the intensity of anti-Yap signature in Tropomyosin positive cells normalized to the Control morpholino group. n = 8 untreated embryos and 15 llgl1 morpholino treated embryos Two-tailed unpaired student’s t-test. (B) qRT-PCR transcript analysis for llgl1, llgl2 and genes regulated by Yap activity in llgl1^{+/+} or llgl1^{-/-} 3 dpf zebrafish hearts. n = 10 for each group. Two-tailed unpaired student’s t-test. (C) Representative images of 3 dpf embryos microinjected with llgl1 morpholino with or without Tol2 mediated integration of myl7:yap-myc. Arrows depict region measured for pericardial effusion. Scale = 1 mm. Quantification of pericardial effusion in 3 dpf embryos. n = 6 uninjected control group, 6 for myl7:yap-myc control group, 7 for llgl1 morphants, and 7 for llgl1 morphants with myl7:yap-myc expression. One-way ANOVA, Tukey’s multiple comparisons test. (D) Quantification of blood flow velocity in 2 dpf embryos. n = 8 uninjected control group, 5 transposase only control group, 5 for myl7:yap-myc control group, 13 for llgl1 morphants, and 9 for llgl1 morphants with myl7:yap-myc expression. One-way ANOVA, Tukey’s multiple comparisons test. *p<0.05, **p<0.01, *p<0.001.”**

Furthermore, we detail Yap-myc and phosphostable Yap-myc expression and their effect on cardiomyocyte proliferation in a previous study which is now referenced in section 3.4. We have updated section 3.4 to reflect the new analysis:

“To assess to what extent the loss of Llgl1 cardiac phenotype was caused by decreased levels of Yap protein, we addressed whether exogenous expression of Yap would rescue heart development in llgl1 morphants. Specifically we microinjected Tol2-based plasmid DNA encoding myc-tagged Yap driven by a cardiomyocyte specific promoter (myl7:Yap-myc). This plasmid was utilized previously and expressed protein was verified at 2 dpf in cardiomyocytes via western blot (Flinn et al., 2019). Interestingly, llgl1^{-/-} embryos were sensitive to microinjection, failing to develop after perturbation at the one-cell stage, thus necessitating the use of the llgl1 morpholino. Exogenous expression of Yap in cardiomyocytes ameliorated the pericardial effusion phenotype of llgl1 morphants at 3 dpf (Fig. 6C). Furthermore, analysis of hemodynamic forces showed a statistically significant increase in blood flow velocity with co- injection of the myl7:Yap-myc construct in llgl1 morphants as compared llgl1 morphants alone (Fig. 6D). No statistical difference in blood flow velocity was observed between in the myl7:Yap- myc treated llgl1 morphants or myl7:Yap-myc treated wildtype embryos and the control groups. This amelioration of deleterious cardiac physiology is consistent with the decrease in Yap protein.”

Supplement

- scale bars are missing from S1, S2B, S5, S6, S7

Author Response: Scale bars have been added to necessary panels.

Discussion

- line 409: "Both loss of Lgl1 in either cultured rat cardiomyocytes or zebrafish epidermis resulted in lower levels of Yap protein and diminished expression of target genes." Gene expression data was only shown for cardiomyocytes (not epidermis), but that the change in gene expression observed in cardiomyocytes upon depletion of Lgl1 depends on Yap was not shown.

Author Response: We now show depletion of *Lgl1* in cultured cardiomyocytes yields a similar depletion of YAP target genes as compared to *Yap* depletion. We additionally now include gene expression data for Yap targets in *llgl1*^{-/-} mutant hearts (Figure 6). This has been clarified in the discussion:

"Nonetheless, we show depletion of Lgl1 in cultured rat cardiomyocytes and zebrafish cardiomyocytes and epidermal cells in vivo resulted in lower levels of total Yap protein. Furthermore, depletion of Lgl1 also resulted in diminished expression of Yap-TEAD target genes in both llgl1^{-/-} mutant zebrafish and cultured rat cardiomyocytes."

- line 431: "composition of apical cell junction factors." This cannot be concluded from EM data.

Author Response: We have revised this statement to better illustrate the aberrant junctions seen between cardiomyocytes or epidermal cells *llgl1* mutants and morphants:

"Similar to the llgl1 morphant retinal neuroepithelium (Clark et al., 2012), we found that apical junctions in the epidermis and intercalated discs in cardiomyocytes of llgl1^{-/-} mutants were elongated and more electron dense as compared to wild-type cells."